Graphene oxide: A glimmer of hope for Assisted Reproductive Technology

Marina Ramal-Sanchez, Luca Valbonetti, Guillaume Tsikis, Florine Dubuisson, Marie-Claire Blache, Valérie Labas, Xavier Druart, Antonella Fontana, Pascal Mermillod, Barbara Barboni, et al.

Title: "Graphene Oxide: a glimmer of hope for Assisted Reproductive Technology"

Authors: Marina Ramal-Sanchez[1,2*], Luca Valbonetti[1], Guillaume Tsikis[2], Florine Dubuisson[2], Marie-Claire Blache[2], Valerie Labas[2,3], Xavier Druart[2], Antonella Fontana[4], Pascal Mermillod[2], Barbara Barboni[1], Marie Saint-Dizier[2,5], Nicola Bernabo[1].

Affiliations:

[1] Faculty of Bioscience and Technology for Food, Agriculture and Environment, Università degli Studi di Teramo, 64100, Teramo, Italy

[2] Physiologie de la Reproduction et des Comportements (PRC) UMR85, INRA, CNRS 7247, IFCE, 37380 Nouzilly, France

[3] Plate-forme de Chirurgie et d'Imagerie pour la Recherche et l'Enseignement (CIRE), Pôle d'Analyse et d'Imagerie des Biomolécules (PAIB), INRA, CHRU de Tours, Université de Tours, 37380 Nouzilly, France.

[4] Department of Pharmacy, University "G. d'Annunzio", 66100, Chieti, Italy

[5] University of Tours, Faculty of Sciences and Techniques, 37200, Tours, France

Running tittle: Graphene Oxide improves IVF efficiency

[1]***Corresponding author** : Marina Ramal-Sanchez, Università degli Studi di Teramo, Campus Coste Sant'Agostino, Via R. Balzarini, 1, 64100 Teramo, Italy; Telf : +39 0861 266836, E-mail : mramalsanchez@unite.it

Abstract

Infertility is a worldwide problem affecting around 48.5 million couples in the word, the male factor being responsible for approximately the 50% of the cases, with a high percentage of unknown causes. For that reason, improving the success of In Vitro Fertilization (IVF) techniques is a primordial aim for researchers working in the reproductive field. Here, by using a mammalian animal model, the bovine, we present an innovative in vitro fertilization system that combines the use of a somatic component, the epithelial oviductal cells, and a carbon-based material, the graphene oxide, with the aim to open new ways in IVF systems design and application.

Our results show an increase in the IVF outcomes without harming the blastocyst developmental rate, as well as high modified proteomic and lipidomic profiles of capacitating spermatozoa. Furthermore, we compared the modifications produced by GO with those exerted by the hormone progesterone, finding similar functional effects on sperm capacitation.

In conclusion, our results stand out the use of a non-physiological material as graphene oxide in a new and innovative strategy that improves sperm capacitation, conferring them a higher fertilizing competence and thus increasing the in vitro fertilization outcomes.

1. Introduction

Male infertility is responsible for approximately the 50% of infertility cases affecting the couples, and among them, around the 40-50% are due to unknown factors (idiopathic male infertility) [1–3]. For that reason, Assisted Reproductive Technology (ART) has acquired an enormous importance in our society since the birth of the first *in vitro* fertilization (IVF) baby in the world, in 1978. Successful fertilization *in vitro* can be achieved performing IVF, in which spermatozoa are co-incubated with the egg, or by intracytoplasmic sperm injection (ICSI), a more invasive treatment in which one sperm cell is injected directly into the oocyte. A recent report from the European IVF-Monitoring (EIM) consortium for the European Society of Human Reproduction and Embryology (ESHRE) showed an increase in the proportion of ICSI (approximately 70% of total fresh cycles) against IVF, although the effectiveness on clinical pregnancy rates stays around the 26-29% for both treatments [4]. However, the use of ICSI has been associated with an increased risk of health issues in mother and children [5,6]. The essential need of improving the success rates of IVF has carried our group into the study of Graphene Oxide (GO) and its potential benefits on sperm capacitation and fertilizing competence acquisition [7].

GO is a carbon-based material characterized by extraordinary properties [8] that have received an increasing attention during the last years due to its interesting applications, extended for example from its use to renewable energy generation [9,10] to the biomedical field [11–14]. Moreover, it had been proposed previously the possibility that GO could exert a detrimental effect on the reproductive function of some animal models [15–19], in particular when spermatozoa are exposed to different GO forms [20–22]. However, recently our group has evaluated the dose-dependent effects of GO on boar sperm function, concretely in some events related to capacitation (*i.e.*,

the ensemble of events that spermatozoa undergo to become fully fertile), revealing a low toxicity level and a positive effect on the IVF outcomes when spermatozoa were capacitated in the presence of GO at a specific concentration (1 µg/mL) [7]. Since our results stand out the potential use of GO to improve the fertilization rates in IVF assays, we adopted in our earlier study an experimental approach in which swine spermatozoa were incubated under capacitating conditions, evidencing the effect of GO on cholesterol extraction from sperm plasma membrane [23], a key event of sperm capacitation. After cholesterol extraction, the sperm membrane undergoes physicochemical modifications, increasing the lipid disorder and the fluidity and enabling the fusion between the plasma membrane (PM) and the outer acrosome membrane (OAM). It is interesting to note also the presence of membrane microdomains called lipid rafts [24], enriched in cholesterol and sphingolipids and involved in the acquisition of fertilizing ability after their reorganization and modification of their protein composition, thus rearranging the signaling machinery [25].

In the present study, we moved on to a more physiological system in which spermatozoa were allowed to interact with the oviductal epithelial cells (OEC). After mating or artificial insemination, spermatozoa reach the oviduct and quickly bind to the oviductal epithelial cells (OECs), where they reside for hours to days in the so called “functional sperm reservoir” [26]. This storage plays an important role in sperm selection [27], maintenance of sperm viability [28], and prevention of premature capacitation [29]. Then, after an uncertain period of time, spermatozoa detach from the oviduct and continue their way towards the fertilization site. The Binder of Sperm Proteins (BSP) -1, -3 and 5 incorporated from the seminal plasma may play important roles in sperm binding to OEC and in the first steps of capacitation by promoting

cholesterol and phospholipids efflux at the time of BSP removal from the sperm membrane [30]. It is of note as well the importance of the ovarian steroid hormone progesterone (P4), naturally present in the female tract during the estrous cycle and which rises its concentration locally within the oviduct around the time of ovulation [31]. P4 can be considered as a sperm releasing factor, inducing the detachment of spermatozoa from oviductal epithelial cells in vivo and in vitro in many species [32–35] and inducing changes not only in the oviductal epithelium but also on spermatozoa [36,37].

The objective of the present study was to elucidate the modifications induced by GO on bovine spermatozoa after the process of binding to OECs and subsequent release from these cells using P4 as a physiological positive control [35,38]. By performing this innovative and complex strategy, we first evaluated the sperm biological function with an IVF approach. Then, to decipher the modifications produced by the GO-induced release, the sperm membrane in terms of membrane fluidity, abundance of BSPs and analysis of lipid rafts composition was analyzed, as well as some sperm intracellular pathways involved in capacitation signaling. Furthermore, we have taken advantage from the recent advances in mass spectrometry in combination with new bioinformatics tools that allow the development of global approaches based on intact cells profiling. Here, Matrix Assisted Laser Desorption/Ionization Time-Of Flight (MALDI-TOF) Mass spectrometry was used directly on isolated spermatozoa to obtain peptidoforms and proteoforms mass fingerprints with a mass range greater than 2,000 m/z for proteins and with a weight range lower than 1,200 m/z for lipids carthography. By using this phenotyping method (ICM-MS) in the last part of this study we moved forward to the molecular level, to evaluate the changes in the lipidomic and proteomic profiles from

the different experimental groups that could help to cast about for some potential biomarkers of sperm capacitation.

2. Materials and Methods

2.1. Materials

Unless otherwise indicated, all chemicals were purchased from Merck-Sigma-Aldrich (Saint Quentin-Fallavier, France).

2.2 Preparation of graphene oxide

Monolayer graphene oxide (GO) was a commercial sample from Graphenea, San Sebastian, Spain, fully characterized by elemental analysis, X-ray Photoelectron Spectroscopy (XPS) spectrum and Transmission Electron Microscopy (TEM). The concentration of the final dispersion was spectrophotometrically checked by using a Cary 100-Bio Varian spectrophotometer and the size of GO flakes in the dispersion were measured at 38.5 °C by Dynamic Laser Light Scattering (90Plus/BI-MAS ZetaPlus multiangle particle size analyzer, Brookhaven Instruments Corp.).

2.3. Bovine spermatozoa collection and processing

Sperm collection and processing was carried out as previously described [35,38]. In brief, a pool of frozen semen from three bulls was used in all the experiments. After thawing, motile spermatozoa were selected through a Percoll (GE Healthcare Life Sciences, Velizy-Villacoublay, France) density gradient (90-45%). The sperm pellet was rinsed and centrifuged at 100 g for 10 min. Sperm motility was visually estimated by light microscopy before each experiment and only samples with a sperm motility >90% were considered in further analyses.

2.4. BOEC collection and co-incubation with bovine spermatozoa

The experimental design is summarized in Figure 1. For the sperm-BOEC co-incubation, different pools of frozen-thawed BOECs were used in the various experiment, as stated earlier [38]. Briefly, both oviducts from 5-7 adult cows at peri-ovulatory stages collected from a local slaughterhouse were dissected and BOECs were gathered by scratching the whole oviducts (ampulla and isthmus tracts), pooled and then rinsed three times in a washing medium (TCM 199 supplemented with Gentamicin 10 mg/mL and BSA 0.2%). BOECs were then diluted 1:10 in a freezing medium (TCM 199 supplemented with DMSO 10%, Gentamicin 10 mg/mL and FBS 20%), aliquoted in cryotubes and stored in liquid nitrogen. For each experiment, an aliquot of BOECs was thawed in a water bath at 34ºC, transferred into a thawing-washing medium (TCM 199 with FBS 20% and Gentamicin 10 mg/mL), washed twice and cultured in 12 well plates (TCM 199 with FBS 20% and Gentamicin 10 mg/mL). After reaching confluence (in 6-7 days of culture post-thawing), BOECs were washed with IVF medium (Tyrode medium supplemented with 25 mM Bicarbonate, 10 mM Lactate, 1 mM Pyruvate, 6 mg/mL fatty acid free BSA, 100 IU/mL Penicillin and 100 µg/mL Streptomycin) and bovine spermatozoa were added to the cells at a final concentration of 4×10^6 sperm cells/mL in the same IVF medium and under culture conditions (humidified atmosphere, 5% CO2, 38.8 °C). After 30 min of co-incubation with BOECs, unbound spermatozoa (BOEC group) were collected and the cells were washed. The release of bound spermatozoa from BOECs was then induced by adding GO (1 µg/mL) to the culture medium for 1 h. The concentration of GO used was previously showed to have beneficial effects on spermatozoa fertilizing ability acquisition [7]. Spermatozoa released from BOECs by GO action (BOEC-GO group) were collected by washing three times with IVF medium. Two control groups of spermatozoa at the same sperm concentration were run in parallel in each experiment: one group in which spermatozoa

were similarly manipulated without BOEC or GO (CTRL group) and another group treated for 1 h GO 1 µg/mL (GO) without BOEC. Moreover, the ability of GO to induce the sperm release was compared with that from P4, used at a concentration of 100 ng/mL (previously reported to be optimal in an earlier study [31]) to induce the sperm release from BOEC (BOEC-P4 group), as well as a group treated for 1 h with P4 (100 ng/mL) (P4 group) without BOEC. After every experiment, the sperm cells-containing supernatants from the unbound group and the spermatozoa released by GO or P4 action were centrifuged for 10 min at 500g and counted by Thoma cell, in order to calculate the percentage of BOEC-GO spermatozoa and evaluate the ability of GO to induce the sperm release from BOECs. As positive controls there were used P4 (100 ng/mL) and heparin (100 µg/mL), this one previously reported to induce the release of ~100% of spermatozoa attached to BOECs monolayers within 1h (BOEC-HEP spermatozoa)[39].

2.5. In vitro fertilization and embryo culture

Bovine oocytes were collected and matured in vitro as previously described [35,40]. Cumulus-oocyte complexes (COCs) were collected from bovine ovaries by aspirating follicles with a diameter of 2-5 mm. COCs surrounded by several layers of compact cumulus cells were selected and washed three times in HEPES-buffered TCM199. Groups of 50 COCs were then transferred into four-well dishes (Nunc, Roskidle, Denmark) and allowed to mature for 22 h in 500 µL of TCM199 supplemented with EGF (10 ng/mL), IGF-1 (19 ng/mL), FGF (2.2 ng/mL), hCG (5 IU/mL), PMSG (10 UI/mL), insulin (5 µg/mL), transferrin (5 µg/mL), selenium (5 ng/mL), L-cystein (90 µg/mL), beta-mercaptoethanol (0.1 mM), ascorbic acid (75 µg/mL), glycine (720 µg/mL), glutamine (0.1 mg/mL) and pyruvate (110 µg/mL) at 38.8°C in a humidified atmosphere with 5% CO_2. At the end of the maturation, COCs were

washed three times in IVF-medium before being transferred in groups of 30-50 oocytes into four-well dishes for insemination.

Spermatozoa and BOECs were prepared and co-incubated as described above. After the co-incubation, BOECs were washed three times with IVF- medium and then the sperm release was induced by incubating with GO (1 µg/mL) or P4 (100 ng/mL) during 1h (BOEC-GO and BOEC- P4 group, respectively). As a control group, spermatozoa were incubated at a final concentration of 4×10^6 spermatozoa/mL in IVF-medium and manipulated by pipetting as the other treated groups and in parallel. The cell supernatant and washing medium from the three experimental groups were centrifuged for 10 min at 100 g before the co-incubation with the oocytes. After determining the sperm concentrations with a Thoma cell, sperm cells at a final concentration of 1×10^6/mL were co-incubated with the in vitro matured oocytes at 38.8°C in 500 µl of IVF-medium containing 10 µg/ml heparin in a humidified atmosphere with 5% CO_2.

Twenty-two hours post-insemination (pi), presumptive zygotes were washed three times in synthetic oviductal fluid [41] to remove cumulus cells and attached spermatozoa. Zygotes were then cultured in 25 µL drops of SOF supplemented with 5 % heat-treated FCS and overlaid with 700 µL of mineral oil. Zygotes were incubated for 8 days at 38.8°C in a humidified atmosphere containing 5% O_2, 5% CO_2 and 90% N_2.

Cleavage rates were determined on Day 2 pi. Blastocyst rates at Days 7 and 8 were determined as percentages of cleaved embryos and hatching rate at Day 8 as percentage of blastocysts at Day 8.

2.6. Evaluation of sperm membrane fluidity by fluorescence recovery after photobleaching (FRAP) analysis

Due to the need of analysing live spermatozoa in a very short length of time, only CTRL, BOEC-GO and BOEC-P4 groups were analysed. FRAP experiments were performed as previously described [38,42]. Briefly, the lipophilic fluorescent molecule DilC12(3) perchlorate (ENZ-52206, Enzo Life Sciences, USA) was added (1:1000) for the last 15 min of the sperm-BOEC co-incubation. Released spermatozoa were then collected and FRAP was carried out within 60 min after collection with a laser-scanning confocal microscope LSM780 (Zeiss, Oberkochen, Germany) with the following acquisition parameters: Plan Apo 63X oil objective, numerical aperture 1.4; zoom 4.2; 1 airy unit; 1 picture every 0.230 sec; fluorescence bleaching and recovery performed at λexc = 561 nm and λem = 595 nm with one scan for basal fluorescence record at 2.4% of the maximum laser power, one scan at 100% laser power for bleaching, and 25 scans for monitoring recovery at 2.4% of the maximum laser power. Recovery curves were obtained and analysed using the simFRAP plug-in for Fiji ImageJ (https://imagej.nih.gov/ij/plugins/sim-frap/index.html, 03/25/2019) [43]. The parameters set were the following: pixel size 0.109 µm; acquisition time per frame 0.095 sec. The results are expressed as diffusion coefficient (cm^2/sec). Six independent experiments were carried out, with an average of 15 spermatozoa analysed per condition and per replicate.

2.7. Evaluation by Western blot of BSP abundance on spermatozoa

Previous studies using the same in vitro system showed that only sperm heads with intact acrosome did bind to the surface of BOECs [35]. In order to reject the hypothesis whereby the release of bound spermatozoa by GO was due to the loss of their acrosome, the integrity of acrosomes in the BOEC-GO and CTRL groups was evaluated using a double staining with PNA (Peanut Agglutinin lectin) and Hoechst 33342 followed by examination under confocal microscopy. Acrosomes were found to

be intact in more than 90% of spermatozoa in both groups (data not shown). For Western-Blot analyses, spermatozoa from all the experimental groups were collected and immediately washed twice in PBS and centrifuged at 2000 g for 3 min before protein extraction. Samples were then diluted in lysis buffer (2% SDS in 10 mM Tris, pH 6.8) with a protease inhibitor cocktail and centrifuged (15000 g for 10 min, 4ºC) to separate the protein-rich supernatant from the cellular debris. The concentration in proteins was assessed in sperm supernatants using the Uptima BC Assay kit (Interchim, Montluçon, France) before dilution in loading buffer (Laemmli buffer 5X) and heating (90ºC for 5 min). Sperm samples extracts were migrated (10 µg of proteins per lane) on a SDS-PAGE 4-15% gradient gel (Mini-PROTEAN® TGX™ Precast Protein Gels, BioRad) and blotted on a nitrocellulose membrane using the Trans-Blot® TurboTM Transfer System (BioRad, Marnes-la-Coquette, France). The membranes were stained with Ponceau S solution (5 min at room temperature, gentle shaking) and scanned with Image Scanner (Amersham Biosciences, GE Healthcare Life Sciences) to check the homogeneous loading among lanes and for normalization (see below). Membranes were blocked in 5% (w/v) milk powder diluted in TBS-T (Tris-buffered saline with 1% (v/v) Tween20) for 1h and then incubated with the primary antibody diluted at 1:1000 (gentle shaking, 4ºC, overnight). Anti-sera against purified bovine BSP-1, BSP-3 and BSP-5 proteins were kindly provided by Dr. Manjunath (Department of Biochemistry and Medicine, Faculty of Medicine, University of Montreal) and antibodies were purified with the Melon Gel IgG spin purification kit (Thermo Fisher Scientific, City, Country), following the supplier's instructions. Blots were finally incubated with fluorescent secondary antibody IRDye® 800CW anti-Rabbit IgG (gently shaking, 37ºC, darkness, 45 min) diluted at 1:10000 before revelation with infrared scanner Odyssey® CLx (LI-

COR Biotechnology, Lincoln, USA). At least three biological replicates were performed for each antibody and each condition.

2.8. Evaluation by Western blot of sperm Ser/Thr phosphorylation by PKA and protein tyrosine phosphorylation

To evaluate PKA activity and tyrosine phosphorylation (pTyr), spermatozoa were diluted in Laemmli buffer 5X, heated (100ºC, 5 min) and centrifuged (15000 g for 10 min at 4ºC). The protein rich supernatant was separated from the cell debris and 1 µL of β-Mercaptoethanol (v/v) was added to each sample. Then, sperm protein extracts without prior quantification were migrated and blotted as stated above. After staining with Ponceau S solution and scanning, the membranes were blocked for 1 h in 5% (w/v) milk powder diluted in TBS-T and incubated with anti-phospho-PKA antibody (Phospho-PKA Substrate (RRXS*/T*), dilution 1:10000 Rabbit mAb, Cell Signaling, Leiden, The Netherlands) in 5% (w/v) BSA in TBS-T (gently shaking, 4ºC, overnight). This antibody detects peptides and proteins containing a phospho-Ser/Thr residue with arginine at the −3 and −2 positions. In this way, it is possible to evaluate the quantity of Ser/Thr phosphorylated residues, as well as the increase of protein tyrosine phosphorylation, giving information about the activation of PKA enzyme. After washing, the membranes were incubated with secondary anti-rabbit HRP (1:5000) antibody for 1 h. The peroxidase was revealed using the Clarity™ Western ECL Blotting Substrates kit from BioRad and the images digitized with a cooled CCD camera (ImageMaster VDS-CL, Amersham Biosciences, GE HealthCare Lifesciences, Pittsburgh, PA). Tyrosine phosphorylation was assessed on the same membranes by stripping the previous antibodies (Stripping solution containing β-mercaptoethanol 43 mM, SDS 1%, Tris HCL 62.5 mM, pH 6.7) at 60ºC for 1 h. After washing, the membranes were blocked in 20% (w/v) bovine gelatine (w/v) in TBS-T for 1 h and

incubated with anti-pTyr antibody (Clone 4G10, dilution 1:10000, Mouse mAb, Merck Millipore, USA) in PBS-T for 90 min. After washing again, the membranes were finally incubated with the secondary anti-Mouse HRP (1:5000) antibody for 1h and revealed as described previously in this section. At least three biological replicates were performed for each antibody and each condition.

2.9. Quantification of Western Blot data

To normalize the data, Ponceau S staining was used, as previously described [44]. Briefly, the whole lanes were quantified by densitometry using the TotalLab Quant software (version 11.4,TotalLab, Newcastle upon Tyne, UK). Protein signals were analyzed by Image Studio™ software (LI-COR Biotechnology, Lincoln, USA) in the case of fluorescent detection (BSP) and with TotalLab Quant software in the case of chemiluminescence detection (PKA and pTyr). The total bands were quantified afterwards using ImageQuantTL (GE Healthcare LifeSciences).

2.10. Statistical analysis of IVF, Western-blot and FRAP data

For statistical analysis, GraphPad Prism 6 Software (La Jolla, CA, USA) was used. Western-blot data were first normalized against Rouge-Ponceau and then BSP data were normalized against the CTRL group (considered at 100%). All data were first subjected to normality test (D'Agostino-Pearson omnibus and Shaphiro-Wilk tests). As Western-blot and FRAP data did not follow a normal distribution, differences between groups were analyzed by the non- parametric Kruskal-Wallis' test followed by Dunn's multiple comparisons tests.

For IVF analysis, the cleavage rates at Day 2 pi were calculated from the total number of COCs. The blastocysts rates at Days 7 and 8, and hatching rates at Day 8 were calculated from the total number of cleaved embryos. Since the system we

analyzed is characterized by a high intrinsic biological variability, we decided to normalize the data with the CTRL, thus we expressed the results obtained in treatment groups as delta % with respect to the CTRL. The rates of development and relative changes between groups were compared by ANOVA followed by Holm-Sidak's multiple comparisons tests (CTRL *vs*. BOEC-P4 and CTRL *vs*. BOEC-GO). . Differences were considered statistically significant when $p<0.05$.

2.11. Sperm proteomic and lipidomic profiling by Intact Cell MALDI-TOF Mass Spectrometry (ICM-MS)

For proteomic and lipidomic analyses, all groups of spermatozoa were washed three times in Tris-Sucrose Buffer (TSB, 20 mM Tris-HCl, 260 mM sucrose, pH 6.8) to remove the culture media and salts. For proteomic profiling, 0.5 µL of saturated CHCA (α-cyano-4-hydroxycinnamic acid) matrix dissolved in 100% ethanol was spotted on a MALDI plate (MTP 384 polished steel) and dried before adding approximately 10^5 spermatozoa (determined using a Thoma cell counting chamber) in one µl and overloading with 2.5 µL of saturated CHCA (α-cyano-4-hydroxycinnamic acid) matrix dissolved in 50% acetonitrile/50% water (v/v) in presence of 0.3% TFA (trifluoroacetic acid). For lipidomic profiling, approximately 2×10^5 spermatozoa in 0.5 µL were spotted and overlaid with 2 µL of DHAP (2,5-dihydroxyacetophenone) matrix at 20 mg/mL solubilized in 90% methanol/10% in presence of 2% TFA. The matrix/sample was allowed to evaporate slowly at room temperature for 30 min before MALDI analysis. For each condition, three biological replicates were performed and for each biological replicate, twenty technical replicates were spotted. Spectra were acquired using a Bruker UltrafleXtreme MALDI-TOF instrument (Bruker Daltonics, Bremen, Germany) equipped with a Smartbeam laser at 2 kHz laser repetition rate following an automated method controlled by FlexControl 3.0 software (Bruker Daltonics, Bremen, Germany).

Spectra were obtained in positive linear ion mode in the 1,000–30,000 m/z (mass/charge) range for proteomics and 100-1,800 m/z range for lipidomics. Each spot was analyzed in triplicate. After external calibration, each spectrum was collected as a sum of 1,000 laser shots in five shot steps (total of 5,000 spectra) with a laser parameter set at medium. To increase mass accuracy (mass error <0.05%), an internal calibration was performed on a mix of cells and calibrant solution (for proteomic, 1µL of calibrant solution containing Glu1-fibrinopeptide B, ACTH (fragment18-39), insulin and ubiquitin, cytochrome C, myoglobin and trypsinogen, while for lipidomic, 1 µL of calibrant solution containing Caffein, MRFA peptide, Leu-Enkephalin, Bradykinine 2–9, Glu1-fibrinopeptide B; reserpine; Bradykinine; Angiotensine I). A lock mass correction was applied to one peak with high peak intensity in all spectra using flexAnalysis 4.0 software (Bruker). For proteomics, the unknown peak at m/z 6821.46 was selected, while for lipidomics, the calibration was achieved with the mass corresponding to the phosphatidylcholine 34:1 (PC 34:1; $[M+H]^+$: 760.5856 m/z).

2.12. Quantification and statistical analysis of ICM-MS data

Spectral processing and analysis were performed with ClinProTools v3.0 software (Bruker Daltonics, Bremen, Germany). The data analysis began with an automated raw data pre-treatment workflow, comprising baseline subtraction (Top Hat, 10% minimum baseline width) and two smoothings using the Savitzky-Golay algorithm. The spectra realignment was performed using prominent peaks (maximal peak shift 2000 ppm, 30% of peaks matching most prominent peaks, exclusion of spectra that could not be recalibrated). Normalization of peak intensity was performed using the Total Ionic Count (TIC) in order to display and compare all spectra on the same scale. Automatic peak detection was applied to the total average spectrum with a signal/background noise greater than 2.

The intra- and inter-experiment variability in measurements were evaluated by a coefficient of variation (CV). For CTRL, BOEC-GO, BOEC-P4 and GO groups, mean CV values did not exceed 18.4%, 23%, 23.1% and 14.4% for proteomics, and 31.3%, 42.6%, 34.5% and 37.8% for lipidomics, respectively. In order to avoid false positives in the differential analyses from the lipidomic analysis due to GO ionization, GO alone with DHAP matrix without spermatozoa was analyzed. Corresponding masses were matched with the differential masses found in the BOEC-GO and GO groups and removed from the lists, discarding finally 7 m/z. Differential analyses between groups (N = 180-200 MALDI spectra per group) were performed using the non-parametric Kruskal-Wallis and Wilcoxon tests for multiple and paired comparisons, respectively. Fold Change (FC) was calculated as the ratio between the mean normalized intensity values. Masses were considered statistically differential between groups if the p-value was < 0.01 with a FC > 1.5 or < 0.67. Receiver operating characteristic (ROC) curves were generated and only masses with areas under the curve (AUCs) > 0.8 were retained. Principal component analysis (PCA) and hierarchical clustering were performed on differential masses using the RStudio Software (RStudio, Boston, MA, USA) (installed packages: *readr, robustbase, caTools, RColorBrewer, MALDIquantForeign, FactoMineR, gplots*).

2.13. ICM-MS data processing for lipid and protein identification

In order to identify the lipids corresponding to the differential peaks obtained by ICM-MS profiling, the masses observed were confronted to a local database created from previous analyses of bovine follicular cells and fluids. This database is a merged list of lipids identified by high resolution mass spectrometry (HRMS) using liquid chromatography coupled with mass spectrometry (LC-MS) and direct infusion for HR-MS/MS structural analyses, as recently described [45]. The comparison of the masses

observed by ICM-MS and the monoisotopic masses identified by HRMS was performed with a max mass tolerance of 0.1 Da for lipids.

In order to identify the proteins corresponding to the differential peaks obtained by ICM-MS profiling, a local database from a previous analysis of ovine spermatozoa by HR-MS/MS coupled to µLC was used. In this analysis, 1 mg of the intact peptides/proteins was subjected to various fractionations through reversed phase and gel filtration chromatographic separations, as previously described [46]. All the data acquired by µLC-HR-MS/MS were automatically processed by the ProSight PC software v4.0 (Thermo Fisher, San Jose, California, USA) [46]. All the data files (*.raw) were processed using the cRAWler application. Molecular weights of precursor and product ions were determined using the xtract algorithm. Automated searches were performed on PUF files using the “Biomarker” search option against a database made from the UniprotKB Swiss-Prot Ovis aries release ovis_aries_2017_07_top_down_complex (28256 sequences, 512072 proteoforms) downloaded from http://proteinaceous.net/database-warehouse/. Iterative search tree was designed for monoisotopic precursors and average precursors at 25 ppm and 2 Da mass tolerance, respectively, and both at 15 ppm for fragment ion level. For all searches, the N-terminal post-translation modifications were considered. Then, all the *.puf files were additionally searched in “Absolute mass” mode using 1000 Da for precursor search window. For identification of endogenous biomolecules, we validated automatically all the peptidoforms/proteoforms with E value $<1E^{-8}$. Furthermore, we validated all hits presenting a C score > 3 [47]. The comparison of the masses observed by ICM-MS and the average masses identified by Top-Down was performed with a max mass tolerance of 0.05% for proteins.

In TD results list, the entry names and gene names were recovered from the UniProtKB accession numbers from *Ovis aries* annotated proteins using the Retrieve/ID mapping of Uniprot (http://www.uniprot.org/uploadlists/) and listed. Proteins identified in *Ovis* were mapped to the corresponding *Bos taurus* taxon by identifying the reciprocal-best-BLAST hits using blastp resource (http://blast.ncbi.nlm.nih.gov/Blast.cgi). Only protein sequences with 100% identity and 100% query cover were retained. The gene name and accession number of identified proteins were recovered from the NCBI database. Protein functions and cellular location were recovered from UniProtKB (Swiss-prot) (https://www.uniprot.org/uniprot/, 03/25/2019) Last, the potential role of proteins identified in membrane lipid rafts was assessed using the RaftProt Database V2 (Mammalian Lipid Raft Proteome Database, http://raftprot.org/, 03/25/2019) by downloading the list of lipid-raft associated proteins detected in bovine experiments (evidence based on Gene Name and UniprotID).

2.14. Protein-protein network creation by STRING

To identify and predict new molecular interactions identifies proteins we used Search Tool for the Retrieval of Interacting Genes/Proteins (STRING) (https://string-db.org/, version 11.0, 03/25/2019) [48]. STRING is a database including known and predicted protein interactions. They could be either direct (physical) or indirect (functional) associations, and are derived from different sources: genomic context, high-throughput experiments, conserved co-expression and previous knowledge. From the data obtained using STRING it was obtained a new network by filtering the data for *bos taurus* species and adopting a medium confidence score (0.400). Afterwards, to identify clusters of molecules within the network, we used the Markov Cluster (MCL) algorithm, setting the inflation parameter (related to the precision of the clustering) at 4.

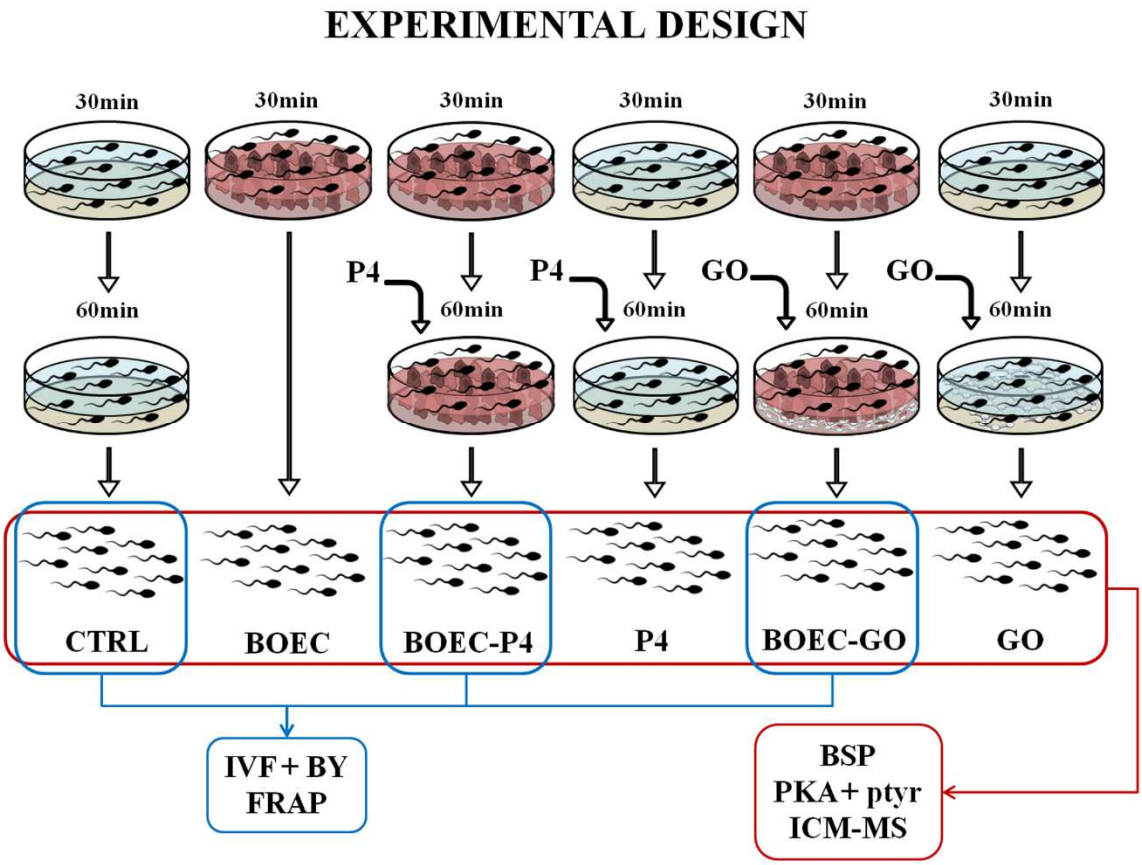

Figure 1. Experimental design. The schema summarizes the experimental design composed by the three main experimental groups and the four control conditions are shown. From left to right: control group (CTRL), spermatozoa unbound (BOEC), spermatozoa released from BOEC by P4 action (BOEC- P4), spermatozoa just treated with P4 without BOEC (P4), spermatozoa released from BOEC by GO action, and just GO-treated spermatozoa without BOEC (GO). All the sperm experimental groups were subjected to BSP, PKA and protein tyrosine phosphorylation analysis by Western Blot, and to lipidomic and proteomic analysis by ICM-MS, while only CTRL, BOEC-P4 and BOEC-GO groups were also used to carry out IVF and blastocyst yield (BY) analysis and FRAP experiments.

3. Results

3.1 Characterization of graphene oxide

Considering the importance of the concentration, lateral size, shape and thickness of GO in their interactions with cells [49], the concentration of the final GO dispersion was spectrophotometrically checked by using the Lambert-Beer law at λ_{max} 230 nm while the dimension of the GO dispersion was checked by Dynamic Laser Light Scattering. The mean diameter of a 1 µg/mL GO dispersion at 38.5 °C is 670±100 nm and the size do not increase on increasing the GO concentration.

3.2. GO induced the release of spermatozoa from BOEC

GO (1 µg/mL) addition to the spermatozoa-BOEC co-culture induced the release of around 65% of spermatozoa previously bound to BOEC, while BOEC-P4 group induced the released of approximately the 50% of bound spermatozoa (see Supplementary Figure 1). These BOEC-GO spermatozoa were subsequently used for IVF and analyzed in the following experiments.

3.3. GO-induced release increased spermatozoa fertilizing competence

As summarized in Table 1, at Day 2 pi the cleavage rates were significantly higher when oocytes were co-incubated with spermatozoa from the BOEC-GO group compared to the CTRL group (84.5% BOEC-GO *vs*. 68.6% for the CTRL, p=0.041). At Days 7 and 8 after IVF, the rates of blastocysts were higher (although not statistically significant) in BOEC-P4 and BOEC-GO groups compared with CTRL, obtaining positive delta values in all the cases, standing out the higher rate and delta of hatching/hatched blastocysts at Day 8.

	COCs	Cleavage (%)	Day-7 blastocysts (%)	Day-8 blastocysts (%)	Hatching Day 8 (%)

		Rate	Delta	Rate	Delta	Rate	Delta	Rate	Delta
CTRL	185	68.6 ± 7.6	-	13.2 ± 5.5	-	17.5 ± 9.6	-	18.3 ± 16.1	-
BOEC-P4	187	75.4 ± 6	9.9	15 ± 7.8	13.6	18.8 ± 7.6	7.4	41.8 ± 8.3	128
BOEC-GO	212	84.5 ± 4.8*	23.2	14.5 ± 6.3	9.8	18.2 ± 6.4	4	34.9 ± 13.4	90

Table 1. In vitro fertilization and embryo development outcomes. Means ± SD of cleavage rate at Day 2, blastocyst rates at Days 7 and 8 pi and hatching rates at Day 8 of bovine embryos after in vitro fertilization with control spermatozoa (CTRL), spermatozoa released from BOEC after P4 (BOEC-P4) and GO (BOEC-GO) action. COCs: total number of cumulus oocyte complexes (COCs); % cleavage from the total COC number; % of blastocyts from the cleaved embryos; % hatching/hatched from the number of blastocyst at Day 8. *Significantly different compared to CTRL ($p<0.05$).

3.4. GO-induced release increased sperm membrane fluidity

Sperm membrane fluidity was assessed by using a FRAP technique. To that, spermatozoa were bleached and then the time to recover the fluorescence was calculated to obtain the diffusion coefficient of the dye DilC12(3). FRAP analysis showed similar increases in the mean diffusion coefficient in BOEC-GO and BOEC-P4 spermatozoa compared to the CTRL group (mean values of 1.38, 3.14 and 3.13 for CTRL, BOEC-P4 and BOEC-GO, respectively, $p=0.014$ for CTRL vs. BOEC-P4 and $p=0.046$ for CTRL vs. BOEC-GO). This difference was due to an increase in membrane fluidity of a subpopulation of spermatozoa released by GO and P4.

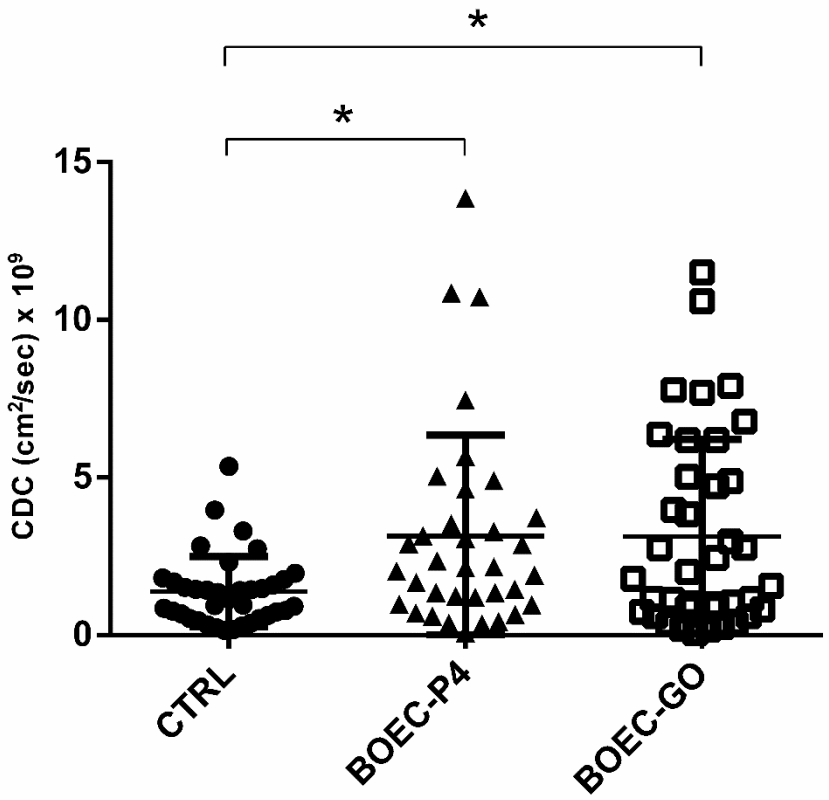

Figure 2. Assessment of sperm membrane fluidity by Fluorescence Recovery After Photobleaching (FRAP). Scatter plot shows calculated diffusion coefficient (CDC) of the dye DilC12(3) in the controls (CTRL), GO-released spermatozoa (BOEC-GO) and P4-released spermatozoa (BOEC-P4). Means and percentiles 25 and 75% are represented (n=6 replicates, *p<0.05).

3.5. GO-induced release decreased BSPs abundance on sperm surface

The mean abundances of membrane proteins BSP-1, BSP-3 and BSP-5 on BOEC-GO spermatozoa were decreased (CTRL:BOEC-GO fold changes of 3.37; 2.94 and 3.48, respectively) while spermatozoa just treated with GO without cells did not present any significant change compared with the CTRL group. Results are similar to those obtained on P4-released and P4-treated spermatozoa (CTRL:BOEC-P4 fold changes of 2.16; 2.89 and 2.76 for BSP-1, BSP-3 and BSP-5, respectively).

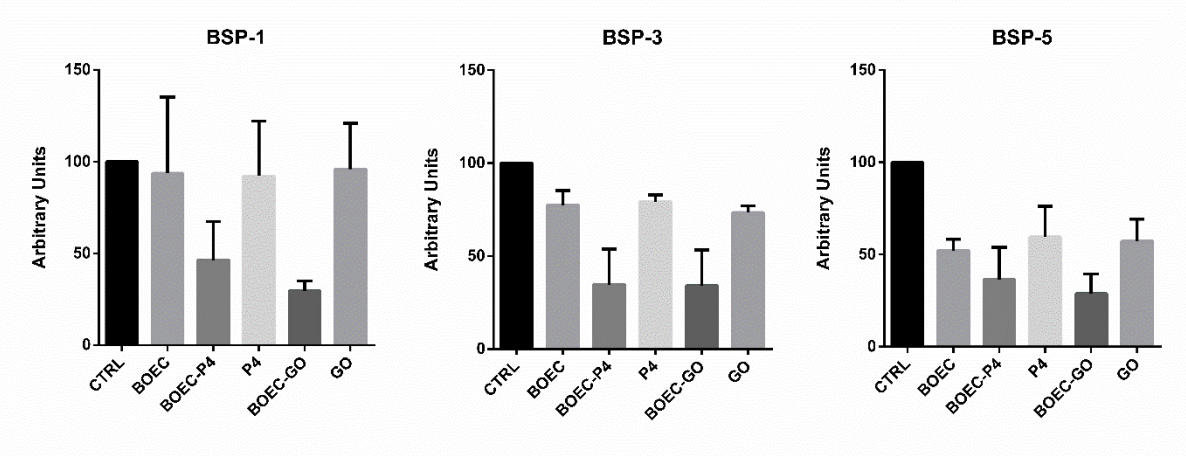

Figure 3. BSP-1, -3, -5 abundance. Histograms exhibit the comparison of BSP-1,-3 and -5 abundance on control spermatozoa (CTRL), spermatozoa unbound or released after a short period of binding and release, spermatozoa released by P4 (BOEC-P4), just-treated P4 spermatozoa (P4), released by GO (BOEC-GO) and just GO-treated (GO) in terms of mean ± SD (n= 3 replicates).

3.6. GO-induced release did not modify sperm PKA activity and pTyr phosphorylation

Although not significant, GO alone tended to increase the levels of phosphorylated Ser/Thr residues by PKA and protein tyrosine (p=0.186 and p=0.383 for PKA and ptyr, respectively) whereas the BOEC-GO group remained at comparable levels of phosphorylation compared with the control group.

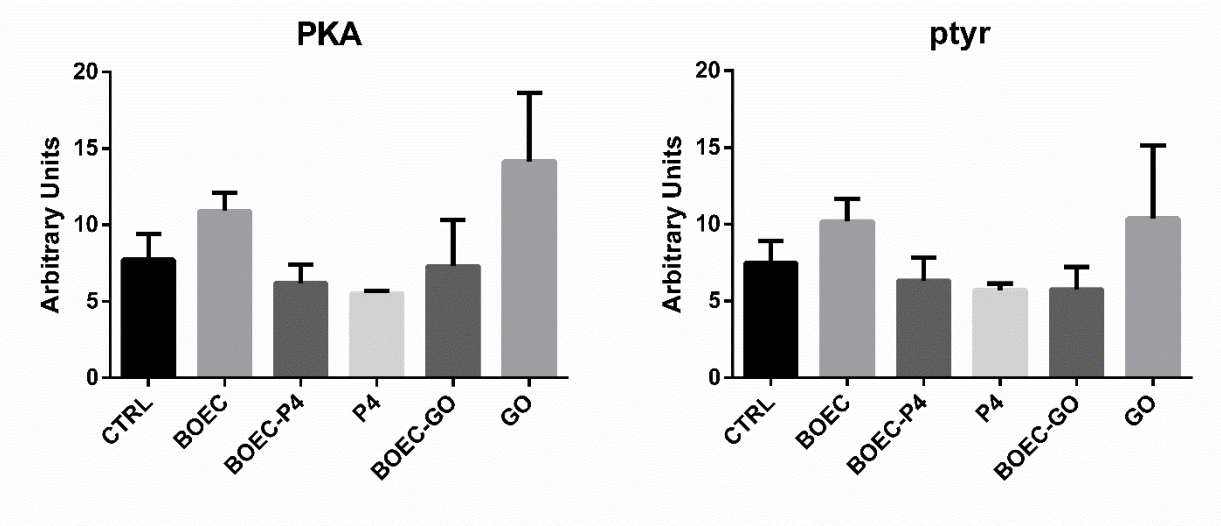

Figure 4. Phosphorylated Ser/Thr residues by PKA and protein tyrosine phosphorylation. (A) Means ± SEM of PKA activity in spermatozoa unbound or released after a short period of binding and release (BOEC), released by P4 after binding (BOEC-P4), just treated by P4 (P4), released by GO after binding (BOEC-GO) and just GO-treated (GO) **(B)** Means ± SEM of protein tyrosine phosphorylation levels in the same groups (n=3 replicates for both histograms, $p>0.05$).

3.7. GO-induced release highly modified sperm lipidomic profiles

A representative spectra of the control group derived from lipidomic analysis is illustrated in Supplementary Material 2 A). After confronting BOEC-GO and GO molecular species with those from the CTRL group, a total of 154 differential m/z were evidenced by ICM-MS. A detailed list with the masses found among each comparison (CTRL Vs BOEC-GO, CTRL Vs. BOEC-P4, CTRL Vs. GO and BOEC-GO Vs. GO) and the criteria to select the differential masses is available in Supplementary Material 3. Amongst these, 144 corresponded to the comparison between BOEC-GO and CTRL groups, while only 8 m/z were differential when comparing GO and CTRL groups (Figure 5A). Furthermore, the differential masses found between CTRL and BOEC-GO groups were compared to those previously obtained between CTRL and BOEC-P4 spermatozoa (Figure 5B). A total of 26 m/z were shared between the two comparisons. GO action on bound spermatozoa modified the sperm lipidomic profiling at a higher level than P4 action (144 vs. 34 m/z). To obtain an overall view of the variations in the peak intensities between the three main experimental conditions (CTRL, BOEC-GO and GO) we performed hierarchical clustering and PCA analysis, in which the different sperm groups were clearly separated (Figure 6A).

3.8. Identification of differential lipids

In total, 67 differential *m/z* were identified, including eight different lipid classes: phosphatidylcholine (PC, 44 m/z), lysophosphatidylcholine (LPC, 12 m/z), triacylglycerol (TG, 9 m/z), shingomyelin (SM, 7 m/z), lysophosphatidylethanolamine (LPE, 2 m/z), ceramide (Cer, 2 m/z), diacylglycerol (DG, 1 m/z) and carnitines (CAR, 1 m/z) (see Supplementary Table 1 for detailed information). It is of note the large proportion of PCs, as PC(36:1) and PC(36:2), that were highly increased in abundance in BOEC-GO spermatozoa compared to controls (BOEC-GO:CTRL fold changes of 18.03 and 14.95, respectively).

3.9. GO-induced release moderately modified sperm proteomic profiles

A representative spectra of the control group derived from proteomic analysis is illustrated in Supplementary Material 2 B). The analysis of proteomic ICM-MS profiles between BOEC-GO, GO and CTRL groups evidenced a total of 156 differential m/z. A detailed list with the masses found among each comparison (CTRL Vs BOEC-GO, CTRL Vs. BOEC-P4, CTRL Vs. GO and BOEC-GO Vs. GO) and the criteria to select the differential masses is available in Supplementary Material 4. The BOEC-GO group showed a total of 91 differential m/z compared to the CTRL group, while the GO group displayed 73 differential m/z. Among these, only 16 m/z where common to both comparisons (Figure 5C). Moreover, when comparing BOEC-GO with previous results obtained for the BOEC-P4 vs. CTRL comparison, a high number of differential molecular species was shared (81 m/z), while 10 and 17 differential m/z were specific to the BOEC-GO vs. CTRL and BOEC-P4 vs. CTRL comparisons, respectively (Figure 5D). As well as for the lipidomic analysis, we illustrated the variations in the m/z peak intensity between the three main experimental conditions (CTRL, BOEC-GO and GO) with hierarchical clustering and PCA analysis, which also show a clear distinct distribution of the sperm groups (Figure 6B).

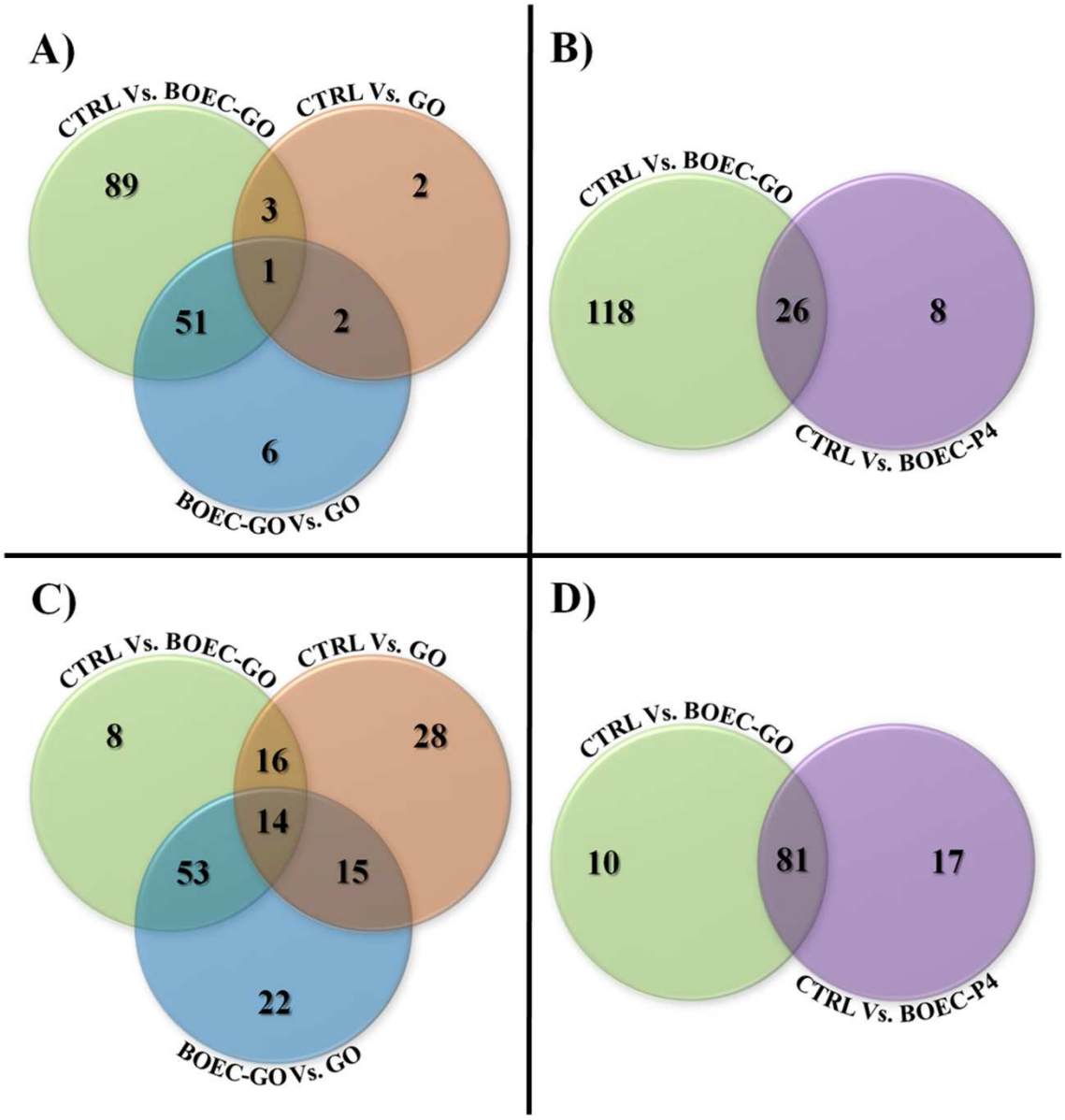

Figure 5. Distribution of differential lipids and proteins between the experimental groups. Venn diagrams confronting the differential *m/z* identified by ICM-MS for lipidomic (A,B) and proteomic (C,D) profiles. CTRL: control spermatozoa; BOEC-GO: spermatozoa bound to BOECs and then released by GO; GO: spermatozoa just treated with GO; BOEC-P4: spermatozoa bound to BOECs and then released by P4 action. (http://bioinformatics.psb.ugent.be/webtools/Venn/).

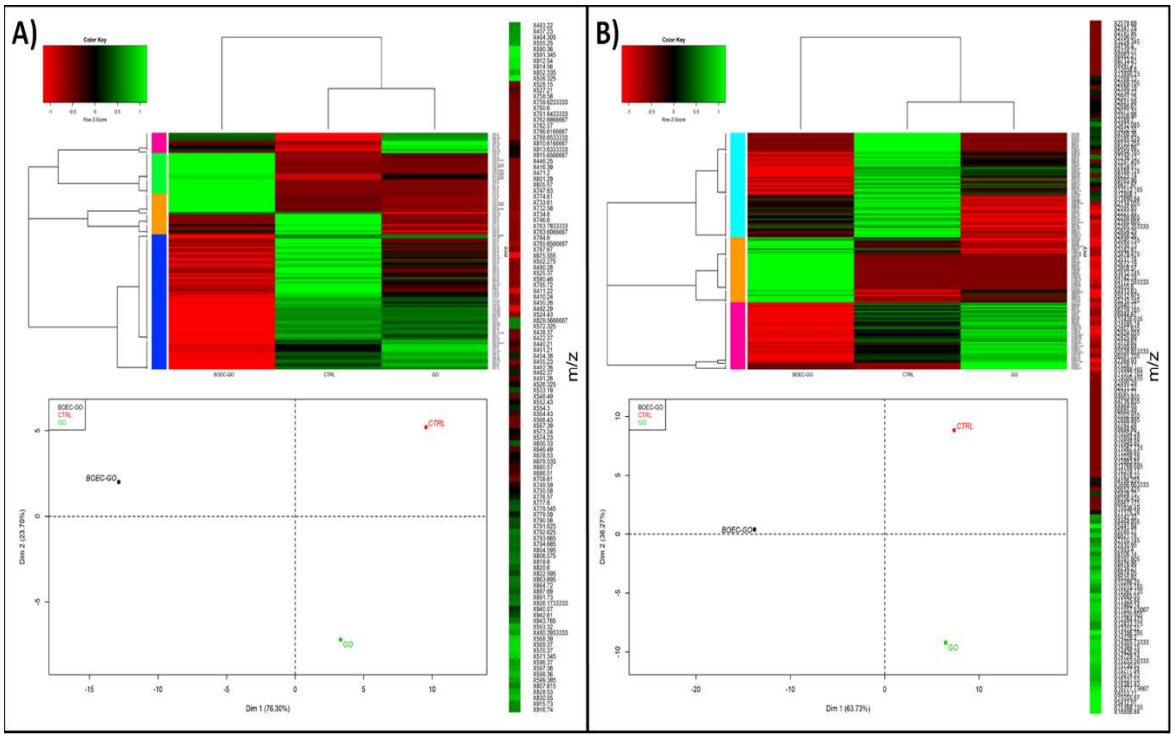

Figure 6. Hierarchical clustering and Principal Component Analysis (PCA) of differential lipids and proteins in spermatozoa. Hierarchical clustering (top) and PCA (bottom) of differentially abundant masses among experimental groups (CTRL, BOEC-GO, GO) for lipidomic (A) and proteomic (B) analyses. CTRL: control spermatozoa; BOEC-GO: spermatozoa bound to BOECs and then released by GO; GO: spermatozoa just treated with GO. For hierarchical clusterings, on the color bar, red is the high spectral count and green is the low count. Patterns of m/z signals were classified into clusters by hierarchical clustering based on different phenotypes of sperm cells. In the PCA chart are represented the three main experimental conditions, symbolizing each one a different population.

3.10. Identification of differential proteins and protein-protein interaction network

A total of 42 differential m/z were identified as peptidoforms from 33 different proteins, among which 8 m/z matched with two possible proteins, and 1 m/z with three proteins. Among the proteins found, five were sperm-specific (SPAM1, ODF3,

SPESP1, bovine proacrosine and Sp17). The biological functions of the proteins found included motility and structural organization, energy and metabolism, signaling, oocyte recognition (ZP binding), stress response, post-translational modification and ATP binding. By using STRING, an online database of known and predicted protein-protein interactions (https://string-db.org/), the direct (physical) and indirect (functional) interactions of those identified proteins between each other and with others are illustrated in Figure 7 (see Supplementary Table 2 for detailed information about the proteins identified).

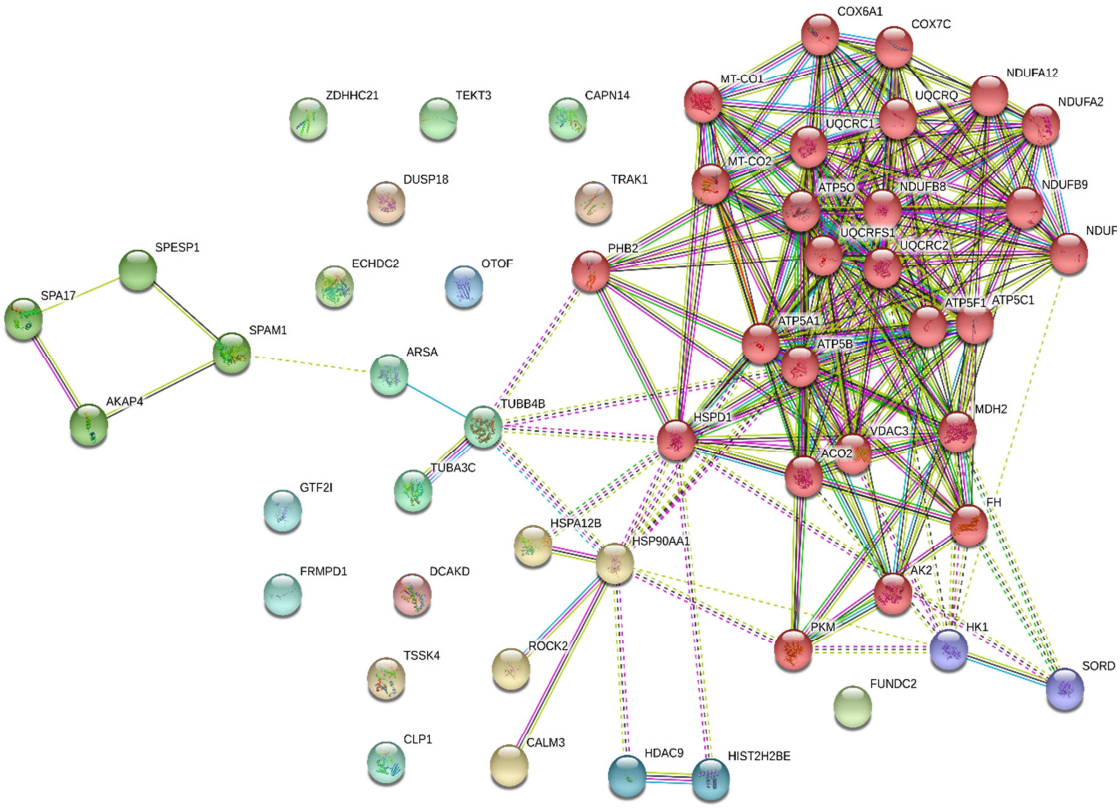

Figure 7. Protein-protein interaction network. Network illustrating the associations between the proteins that matched with the peptidoforms identified (https://string-db.org/)

4. Discussion

Over the last decades, ART has acquired a great importance in our society to fulfill the wish of many infertile couples with the use of IVF and ICSI techniques. However, the more invasive ICSI technique is gaining ground to IVF method, entailing a series of problems not only for the mother (placental abruption, pre-eclampsia and stillbirths) but also for the babies (development of tumors and carcinomas, congenital anomalies such as septal heart defects and cleft lip or palate, as well as neurological problems that may result in an intellectual lag) [5,6]. For this reason, improving the success rates of IVF techniques is a primordial aim for ART, in order to overcome the use of IVF versus ICSI in the near future. To that aim, we have developed an IVF approach in which we include oviductal epithelial cells as a somatic component naturally present in vivo, and GO, a promising carbon-based material with great potential applications in medicine.

Here, we illustrate some events related to sperm capacitation, a key process common to many species and indispensable to achieve a successful fertilization. This ensemble of events are played out either in vivo during the sperm migration within the female genital tract, especially in the oviduct, or in vitro, induced by the presence of some ions and proteins as HCO_3^-, Ca^{2+} and serum albumin [50]. Interestingly, we found that GO (1 µg/mL) addition to the spermatozoa-BOECs co-culture induced the release of almost the 65% of spermatozoa previously bound to BOEC.

First, we assessed the sperm fertilizing ability of bovine spermatozoa after GO-induced release from BOEC by an IVF assay. The positive effect of GO treatment on the cleavage rate was in accordance with previous results observed in a swine model [7] and we were able in this study to confirm a positive rate of blastocysts development, denoting the absence of toxicity and a potential beneficial effect when bull spermatozoa

were incubated with GO in vitro. It is noteworthy as well the higher (although not statistically significant) rate of hatching/hatched blastocysts obtained when using BOEC-GO spermatozoa compared to the control group, since elevated hatching rates have been related to better implant potential and developing into a positive pregnancy in humans [51].

In that way, we started our analysis evaluating the sperm membrane state. It is well accepted (although controversial [52,53]) that spermatozoa are transcriptionally silent and with a limited lipid metabolism, with virtually no cytosol (thus numerous molecules involved in sperm signaling are localized in the membrane), pointing out the central role of the membrane during the process of acrosome reaction [54]. During capacitation, numerous membrane lipids are displaced, increasing the membrane fluidity and modulating the activity of several enzymes and proteins, leading to a deep remodeling of the membranes. Here, by using an already validated FRAP approach [42], we evidenced an increase in the membrane fluidity of some spermatozoa released from BOECs, probably caused by the extraction of cholesterol by GO [23], one of the events responsible for the beginning of capacitation. In order to appraise the results obtained, we compared the calculated diffusion coefficients (CDC) with those obtained when using P4, considered as a physiological stimulus. The results show similar levels of CDC on BOEC-GO and BOEC-P4 spermatozoa, translated into an alike increase in membrane fluidity. This result suggests that GO and P4 could be able to modify the membrane composition by arrangement of the lipids present in the inner and outer leaflet membrane, thus probably participating in the detachment from the oviductal cells. In addition to the FRAP experiments, we studied the abundance of Binder of Sperm Proteins 1, 3 and 5 (BSP-1,-3,-5) on sperm surface with and without induced release. These proteins from the seminal plasma are known to have a role on sperm

binding to OEC and to participate in the first steps of capacitation by promoting cholesterol and phospholipids efflux after their removal from the sperm membrane. Our results, similar to those obtained on BOEC-P4 [38], show a sharp decrease in BSP-1, -3 and -5 abundance on sperm surface, in accordance with the increase in the membrane fluidity evidenced by the FRAP analysis. These results suggest that similar to P4, GO acts interacting with spermatozoa, producing some modifications that somehow leads to an increase in the membrane fluidity and finally to the acquisition of a higher fertilizing competence.

The sperm function is strictly dependent on the composition of the membrane, forasmuch as the changes undergone activate some membrane and cytosolic proteins and enzymes that will trigger the signaling pathways involved in the acquisition of sperm fertilizing ability. Lipids rafts are membrane microdomains enriched in sterols and sphingolipids where are embedded important proteins that regulate intracellular function and cell signaling [24]. Since cholesterol is necessary for the stabilization of the lipid rafts, and the phospholipid composition changes during the remodeling of the membrane [55], the amount, distribution or composition of lipid rafts might be affected by the GO-induced release, as well as the membrane proteins and receptors embedded on them. In this work, by ICM-MS, we found by proteomic analysis eight peptides corresponding to proteins related to bovine lipid rafts (VDAC3, HSP90AA1, TUBB4B, UQCRC1, ATP5F1B, H2B, PHB2, UQCRFS1), which play interesting roles in sperm signaling and whose increase or decrease in BOEC-GO spermatozoa could be linked to the lipid remodeling. In addition, it is noteworthy that, even if we found some similar results in BOEC-P4 spermatozoa in terms of membrane fluidity, the number of differential masses (m/z) derived from lipidomic analysis, especially of PCs and SMs, was substantially higher in BOEC-GO spermatozoa compared to BOEC-P4 (144 vs 34

m/z). Given that GO has a hydrophilic nature, it is able to interact by the oxygen atoms with the positive charge of the phosphorus atom in the phosphate group [56], probably explaining the greater number of differential m/z obtained from lipidomic analysis compared to BOEC-P4 spermatozoa.

In this work, 33 proteins were identified from the differential masses evidenced in the proteomic profile (see Supplementary Table 2), among which six (SORD, AKAP-4, HSPD1, FH, ACO2, TUBA3C) were increased in BOEC-GO spermatozoa compared to controls. It is remarkable the great number of specific differential peptides found decreased on the GO group compared to CTRL, while this decrease was modulated on the BOEC-GO group, illustrating the role of the oviductal cells in the modulation of the sperm proteomics in the binding-release process, presumably preventing sperm cells from a premature capacitation. This results support our experimental model as a good strategy to study GO-sperm interactions in a more physiological environment.

Among the peptidoforms found, most of them corresponded to proteins with a role in sperm motility and structural organization, or involved in metabolism pathways and energy production. Within the latter we found peptides corresponding to COX6A1, MDH2 and NADH proteins (2184.01, 2392.24 and 3387.66 Da, respectively) that were decreased on BOEC-GO spermatozoa compared with controls (fold changes of 0.44, 0.58 and 0.55, respectively). By the other hand, the fragment from protein ACO2 (3177.6 Da), an important enzyme from the tricarboxylic acid (TCA) cycle that contributes to ATP production was found to be increased in BOEC-GO spermatozoa (fold change of 1.69 compared with controls). These results are in concordance with earlier studies showing a decreased level of total ACO2 protein in sperm cells from asthenozoospermic patients compared to normal fertile men [57]. Along the same line we found a fragment from the SORD protein (3383.94 Da) highly increased in the

BOEC-GO group (fold change 5.74 compared with controls). SORD is an enzyme responsible for the oxidizing of sorbitol to fructose using NAD^+ and has been reported to participate in sperm motility and protein tyrosine phosphorylation [58].

It is outstanding as well the presence of calmodulin (CALM), localized in the acrosome and the flagellum and that plays an important role on sperm capacitation and acrosome reaction by increasing the intracellular Ca2+ concentrations necessary for the sperm normal and hyperactivated motility [59]. CALM protein contains EF-hand domains that change their conformation after Ca2+ binding, leading to the activation or inactivation of target proteins. In this work, three molecular species obtained from the proteomic analysis were peptides from the EF-hand domains [60,61] of CALM (10513.8, 4855.7 and 4913.6 Da). CALM/Ca2+ complex, due to the exposure of hydrophobic and less negatively charge surface, has been shown to assemble GO with strong hydrophobic interaction and weak electrostatic repulsion [62]. The adsorption of the proteins onto the GO surface could stabilize their native structures or even induce conformational changes or alterations, affecting in this way the functionality or biological activity of the protein [63].

The changes experienced in the membrane, together with the increased intracellular concentration of diverse factors and some proteins modifications trigger the activation of multiple signaling events and pathways. Hence, in this work we focus our attention in one of the signaling pathways that entail PKA activation and protein tyrosine phosphorylation in spermatozoa. PKA enzyme is a tetrameric protein consisting in two regulatory and two catalytic subunits that could be activated by cAMP binding to the regulatory subunit, releasing the catalytic portions that have the ability to phosphorylate diverse specific proteins (thus phosphorylating tyrosine residues from a variety of proteins), initiating a cascade of intracytoplasmic signaling events in the

sperm cell. It is interesting to note that PKA enzyme is able to bind A-kinase anchoring proteins (AKAPs), and mostly AKAP-3 and -4, to the regulatory subunit of the protein. AKAP-4 (whose peptide at 4960.6 Da from our analysis was found increased in the BOEC-GO group with a fold change of 3.67, compared to the CTRL group) is the major component of sperm fibrous sheaths and possesses the ability to form molecular complexes with other signaling proteins. The amphipathic helix of AKAP4 constitutes a specific PKA-binding domain, participating in this way to the regulation of PKA phosphorylating activity. Our results show no significant differences regarding PKA activation or protein tyrosine phosphorylation, therefore hypothesizing that GO does not induce any detrimental effect in this signaling pathway and that the main responsibility for the increased sperm fertilizing competence relies on the sperm membrane modifications.

Interestingly, in the present work we compared the effects derived from the use of GO with those induced by P4 after the release from BOECs, obtaining similar functional effects on both experimental groups with slight differences at the molecular level, mainly related to the hydrophobic nature of GO that could highly modify the sperm membrane. We are aware about the limitations of the bovine model to study the possible epigenetic changes derived from the use of GO, as previously stated [18,19]. However, although further research is still needed, these results could be interesting to consider, given that GO could act as a substitute of P4 in some special cases in order to avoid the difficulty of using P4 in vitro and the problems associated to its lipid and steroid nature (since the hormone is derived from cholesterol [64]) reaching the same positive effects overall in the IVF outcomes.

5. Conclusions

In conclusion, by using a mammalian in-vitro model, we designed in this work an innovative strategy that turns out to increase the IVF outcomes. By simulating in vitro the sperm reservoir naturally formed within the oviduct, we characterized the modifications induced by GO on bull spermatozoa after their released from OECs. The results obtained emphasize the role played by GO as a sperm releasing factor, stimulating fertilizing ability by increasing the sperm membrane fluidity and modifying the sperm lipidomic and proteomic profiles, without affecting PKA signaling pathway. Moreover, we found that GO has similar functional effects than P4 on sperm capacitation. Taken together, our results highlight for the first time the potential benefit of using graphene oxide in the field of ART.

Authors' contributions

MRS, NB, and MSD conceived the work; all authors curated the data; NB, MSD and MRS performed the formal analysis; AF prepared and characterized GO solution; NB and BB obtained the funding; MRS performed cell culture experiments; MRS and MCB performed and analyzed FRAP experiments; MRS, VL and XD performed and analyzed mass spectrometry experiments; MRS, PM and FD performed and analyzed IVF experiments; MRS, GT and XD performed and analyzed Western Blot experiments; LV created and edited all manuscript figures; NB, BB, PM and MSD administered the project and provided the resources; NB, MSD, BB and PM supervised the work; all authors validated the data; MRS and NB wrote the original draft with the involvement of all the co-authors; MSD critically corrected the draft; all authors reviewed and edited the manuscript; all authors approved the final version of the present manuscript.

Acknowledgements

MRS work was supported by MSCA-ITN Horizon 2020, Project REP-BIOTECH 675526. The authors thank Emilie Corbin and Peggy Jarrier from INRA (Nouzilly, France) for their technical support in oviductal cell collection and culture. This work has as well benefited from the facilities and expertise of the "Plateforme d'imagerie Cellulaire" (PIC) of the UMR-PRC (INRA- Centre Val de Loire).

References

[1] T.K. Jensen, R. Jacobsen, K. Christensen, N.C. Nielsen, E. Bostofte, Good semen quality and life expectancy: a cohort study of 43,277 men., Am. J. Epidemiol. 170 (2009) 559–65. doi:10.1093/aje/kwp168.

[2] J.D. Ring, A.A. Lwin, T.S. Köhler, Current medical management of endocrine-related male infertility., Asian J. Androl. 18 (2016) 357–63. doi:10.4103/1008-682X.179252.

[3] B.R. Winters, T.J. Walsh, The epidemiology of male infertility., Urol. Clin. North Am. 41 (2014) 195–204. doi:10.1016/j.ucl.2013.08.006.

[4] A.P. Ferraretti, K. Nygren, A.N. Andersen, J. de Mouzon, M. Kupka, C. Calhaz-Jorge, C. Wyns, L. Gianaroli, V. Goossens, Trends over 15 years in ART in Europe: an analysis of 6 million cycles†, Hum. Reprod. Open. 2017 (2017). doi:10.1093/hropen/hox012.

[5] M.J. Sánchez-Calabuig, A.P. López-Cardona, R. Fernández-González, P. Ramos-Ibeas, N. Fonseca Balvís, R. Laguna-Barraza, E. Pericuesta, A. Gutiérrez-Adán, P. Bermejo-Álvarez, Potential Health Risks Associated to ICSI: Insights from Animal Models and Strategies for a Safe Procedure., Front. Public Heal. 2 (2014) 241. doi:10.3389/fpubh.2014.00241.

[6] P.J. Bridges, M. Jeoung, H. Kim, J.H. Kim, D.R. Lee, C. Ko, D.J. Baker, Methodology matters: IVF versus ICSI and embryonic gene expression., Reprod. Biomed. Online. 23 (2011) 234–44. doi:10.1016/j.rbmo.2011.04.007.

[7] N. Bernabò, A. Fontana, M.R. Sanchez, L. Valbonetti, G. Capacchietti, R. Zappacosta, L. Greco, M. Marchisio, P. Lanuti, E. Ercolino, B. Barboni, Graphene oxide affects in vitro fertilization outcome by interacting with sperm membrane in an animal model, Carbon N. Y. 129 (2018) 428–437. doi:10.1016/J.CARBON.2017.12.042.

[8] A.K. Geim, Graphene: status and prospects., Science. 324 (2009) 1530–4. doi:10.1126/science.1158877.

[9] J. Kusuma, R.G. Balakrishna, S. Patil, M.S. Jyothi, H.R. Chandan, R. Shwetharani, Exploration of graphene oxide nanoribbons as excellent electron conducting network for third generation solar cells, Sol. Energy Mater. Sol. Cells. 183 (2018) 211–219. doi:10.1016/J.SOLMAT.2018.01.039.

[10] L. Liu, K. Zheng, Y. Yan, Z. Cai, S. Lin, X. Hu, Graphene Aerogels Enhanced Phase Change Materials prepared by one-pot method with high thermal conductivity and large latent energy storage, Sol. Energy Mater. Sol. Cells. 185 (2018) 487–493. doi:10.1016/J.SOLMAT.2018.06.005.

[11] K. Tadyszak, J. Wychowaniec, J. Litowczenko, K. Tadyszak, J.K. Wychowaniec, J. Litowczenko, Biomedical Applications of Graphene-Based Structures, Nanomaterials. 8 (2018) 944. doi:10.3390/nano8110944.

[12] Y.C. Shin, S.-J. Song, S.W. Hong, J.-W. Oh, Y.-S. Hwang, Y.S. Choi, D.-W. Han, Graphene-Functionalized Biomimetic Scaffolds for Tissue Regeneration, in: Springer, Singapore, 2018: pp. 73–89. doi:10.1007/978-981-13-0445-3_5.

[13] D. Chen, C.A. Dougherty, K. Zhu, H. Hong, Theranostic applications of carbon nanomaterials in cancer: Focus on imaging and cargo delivery, J. Control. Release. 210 (2015) 230–245. doi:10.1016/J.JCONREL.2015.04.021.

[14] R. Jha, P.K. Jha, S. Gupta, S.P. Bhuvaneshwaran, M. Hossain, S.K. Guha, Probing suitable therapeutic nanoparticles for controlled drug delivery and diagnostic reproductive health biomarker development, Mater. Sci. Eng. C. 61 (2016) 235–245. doi:10.1016/j.msec.2015.12.044.

[15] N. Chatterjee, Y. Kim, J. Yang, C.P. Roca, S.-W. Joo, J. Choi, A systems toxicology approach reveals the Wnt-MAPK crosstalk pathway mediated reproductive failure in *Caenorhabditis elegans* exposed to graphene oxide (GO) but not to reduced graphene oxide (rGO), Nanotoxicology. 11 (2017) 76–86. doi:10.1080/17435390.2016.1267273.

[16] N.K. Nirmal, K.K. Awasthi, P.J. John, Effects of Nano-Graphene Oxide on Testis, Epididymis and Fertility of Wistar Rats, Basic Clin. Pharmacol. Toxicol. 121 (2017) 202–210. doi:10.1111/bcpt.12782.

[17] J.P. Souza, F.P. Venturini, F. Santos, V. Zucolotto, Chronic toxicity in Ceriodaphnia dubia induced by graphene oxide, Chemosphere. 190 (2018) 218–224. doi:10.1016/j.chemosphere.2017.10.018.

[18] E. Hashemi, O. Akhavan, M. Shamsara, R. Rahighi, A. Esfandiar, A.R. Tayefeh, Cyto and genotoxicities of graphene oxide and reduced graphene oxide sheets on spermatozoa, RSC Adv. 4 (2014) 27213. doi:10.1039/c4ra01047g.

[19] E. Hashemi, O. Akhavan, M. Shamsara, M. Daliri, M. Dashtizad, A. Farmany, Synthesis and cyto-genotoxicity evaluation of graphene on mice spermatogonial stem cells, Colloids Surfaces B Biointerfaces. 146 (2016) 770–776.

doi:10.1016/J.COLSURFB.2016.07.019.

[20] W. Asghar, H. Shafiee, V. Velasco, V.R. Sah, S. Guo, R. El Assal, F. Inci, A. Rajagopalan, M. Jahangir, R.M. Anchan, G.L. Mutter, M. Ozkan, C.S. Ozkan, U. Demirci, Toxicology Study of Single-walled Carbon Nanotubes and Reduced Graphene Oxide in Human Sperm, Sci. Rep. 6 (2016) 30270. doi:10.1038/srep30270.

[21] T. Mesarič, K. Sepčić, D. Drobne, D. Makovec, M. Faimali, S. Morgana, C. Falugi, C. Gambardella, Sperm exposure to carbon-based nanomaterials causes abnormalities in early development of purple sea urchin (Paracentrotus lividus), Aquat. Toxicol. 163 (2015) 158–166. doi:10.1016/j.aquatox.2015.04.012.

[22] S. Liang, S. Xu, D. Zhang, J. He, M. Chu, Reproductive toxicity of nanoscale graphene oxide in male mice, Nanotoxicology. 9 (2015) 92–105. doi:10.3109/17435390.2014.893380.

[23] N. Bernabo, J. Machado-Simoes, L. Valbonetti, M. Ramal-Sanchez, G. Capacchietti, A. Fontana, R. Zappacosta, P. Palestini, L. Botto, M. Marchisio, P. Lanuti, M. Ciulla, A. Di Stefano, E. Fioroni, M. Spina, B. Barboni, Graphene Oxide increases mammalian spermatozoa fertilizing ability by extracting cholesterol from their membranes and promoting capacitation, (2019) Submitted manuscript.

[24] N. Kawano, K. Yoshida, K. Miyado, M. Yoshida, Lipid rafts: keys to sperm maturation, fertilization, and early embryogenesis., J. Lipids. 2011 (2011) 264706. doi:10.1155/2011/264706.

[25] L. Botto, N. Bernabò, P. Palestini, B. Barboni, Bicarbonate Induces Membrane Reorganization and CBR1 and TRPV1 Endocannabinoid Receptor Migration in

Lipid Microdomains in Capacitating Boar Spermatozoa, J. Membr. Biol. 238 (2010) 33–41. doi:10.1007/s00232-010-9316-8.

[26] S.S. Suarez, Mammalian sperm interactions with the female reproductive tract, Cell Tissue Res. 363 (2016) 185–194. doi:10.1007/s00441-015-2244-2.

[27] P. Tienthai, The porcine sperm reservoir in relation to the function of hyaluronan., J. Reprod. Dev. 61 (2015) 245–50. doi:10.1262/jrd.2015-006.

[28] J.E. Ellington, J.C. Samper, A.E. Jones, S.A. Oliver, K.M. Burnett, R.W. Wright, In vitro interactions of cryopreserved stallion spermatozoa and oviduct (uterine tube) epithelial cells or their secretory products., Anim. Reprod. Sci. 56 (1999) 51–65. http://www.ncbi.nlm.nih.gov/pubmed/10401702 (accessed October 30, 2018).

[29] S.C. Murray, T.T. Smith, Sperm interaction with fallopian tube apical membrane enhances sperm motility and delays capacitation., Fertil. Steril. 68 (1997) 351–7. http://www.ncbi.nlm.nih.gov/pubmed/9240269 (accessed October 30, 2018).

[30] G. Plante, B. Prud'homme, J. Fan, M. Lafleur, P. Manjunath, Evolution and function of mammalian binder of sperm proteins, Cell Tissue Res. 363 (2016) 105–127. doi:10.1007/s00441-015-2289-2.

[31] J. Lamy, P. Liere, A. Pianos, F. Aprahamian, P. Mermillod, M. Saint-Dizier, Steroid hormones in bovine oviductal fluid during the estrous cycle, Theriogenology. 86 (2016) 1409–1420. doi:10.1016/j.theriogenology.2016.04.086.

[32] T. Ito, N. Yoshizaki, T. Tokumoto, H. Ono, T. Yoshimura, A. Tsukada, N. Kansaku, T. Sasanami, Progesterone Is a Sperm-Releasing Factor from the

Sperm-Storage Tubules in Birds, Endocrinology. 152 (2011) 3952–3962. doi:10.1210/en.2011-0237.

[33] R.H.F. Hunter, Sperm release from oviduct epithelial binding is controlled hormonally by peri-ovulatory graafian follicles, Mol. Reprod. Dev. 75 (2008) 167–174. doi:10.1002/mrd.20776.

[34] R.H.F. Hunter, Components of oviduct physiology in eutherian mammals, Biol. Rev. 87 (2012) 244–255. doi:10.1111/j.1469-185X.2011.00196.x.

[35] J. Lamy, E. Corbin, M.-C. Blache, A.S. Garanina, R. Uzbekov, P. Mermillod, M. Saint-Dizier, Steroid hormones regulate sperm–oviduct interactions in the bovine, Reproduction. 154 (2017) 497–508. doi:10.1530/REP-17-0328.

[36] P. V. Lishko, I.L. Botchkina, Y. Kirichok, Progesterone activates the principal Ca2+ channel of human sperm, Nature. 471 (2011) 387–391. doi:10.1038/nature09767.

[37] H.A. Guidobaldi, M.E. Teves, D.R. Uñates, A. Anastasía, L.C. Giojalas, Progesterone from the Cumulus Cells Is the Sperm Chemoattractant Secreted by the Rabbit Oocyte Cumulus Complex, PLoS One. 3 (2008) e3040. doi:10.1371/journal.pone.0003040.

[38] M. Ramal Sanchez, N. Bernabo, G. Tsikis, M.-C. Blache, V. Labas, X. Druart, P. Mermillod, M. Saint-Dizier, Progesterone induces sperm release from bovine oviductal epithelial cells by modifying sperm proteomics, lipidomics and membrane fluidity, (2019) Submitted manuscript.

[39] R. Talevi, R. Gualtieri, Sulfated Glycoconjugates Are Powerful Modulators of Bovine Sperm Adhesion and Release from the Oviductal Epithelium In Vitro1,

Biol. Reprod. 64 (2001) 491–498. doi:10.1095/biolreprod64.2.491.

[40] A. Cordova, C. Perreau, S. Uzbekova, C. Ponsart, Y. Locatelli, P. Mermillod, Development rate and gene expression of IVP bovine embryos cocultured with bovine oviduct epithelial cells at early or late stage of preimplantation development, Theriogenology. 81 (2014) 1163–1173. doi:10.1016/J.THERIOGENOLOGY.2014.01.012.

[41] P. Holm, P.J. Booth, M.H. Schmidt, T. Greve, H. Callesen, High bovine blastocyst development in a static in vitro production system using sofaa medium supplemented with sodium citrate and myo-inositol with or without serum-proteins, Theriogenology. 52 (1999) 683–700. doi:10.1016/S0093-691X(99)00162-4.

[42] N. Bernabò, L. Valbonetti, L. Greco, G. Capacchietti, M. Ramal Sanchez, P. Palestini, L. Botto, M. Mattioli, B. Barboni, Aminopurvalanol A, a Potent, Selective, and Cell Permeable Inhibitor of Cyclins/Cdk Complexes, Causes the Reduction of in Vitro Fertilizing Ability of Boar Spermatozoa, by Negatively Affecting the Capacitation-Dependent Actin Polymerization., Front. Physiol. 8 (2017) 1097. doi:10.3389/fphys.2017.01097.

[43] D. Blumenthal, L. Goldstien, M. Edidin, L.A. Gheber, Universal Approach to FRAP Analysis of Arbitrary Bleaching Patterns., Sci. Rep. 5 (2015) 11655. doi:10.1038/srep11655.

[44] I. Romero-Calvo, B. Ocón, P. Martínez-Moya, M.D. Suárez, A. Zarzuelo, O. Martínez-Augustin, F.S. de Medina, Reversible Ponceau staining as a loading control alternative to actin in Western blots, Anal. Biochem. 401 (2010) 318–320. doi:10.1016/j.ab.2010.02.036.

[45] P. Bertevello, A.-P. Teixeira-Gomes, A. Seyer, A. Vitorino Carvalho, V. Labas, M.-C. Blache, C. Banliat, L. Cordeiro, V. Duranthon, P. Papillier, V. Maillard, S. Elis, S. Uzbekova, Lipid Identification and Transcriptional Analysis of Controlling Enzymes in Bovine Ovarian Follicle, Int. J. Mol. Sci. 19 (2018) 3261. doi:10.3390/ijms19103261.

[46] L. Soler, V. Labas, A. Thélie, I. Grasseau, A.-P. Teixeira-Gomes, E. Blesbois, Intact Cell MALDI-TOF MS on Sperm: A Molecular Test For Male Fertility Diagnosis, Mol. Cell. Proteomics. 15 (2016) 1998–2010. doi:10.1074/mcp.M116.058289.

[47] R.D. LeDuc, R.T. Fellers, B.P. Early, J.B. Greer, P.M. Thomas, N.L. Kelleher, The C-Score: A Bayesian Framework to Sharply Improve Proteoform Scoring in High-Throughput Top Down Proteomics, J. Proteome Res. 13 (2014) 3231–3240. doi:10.1021/pr401277r.

[48] D. Szklarczyk, A. Franceschini, S. Wyder, K. Forslund, D. Heller, J. Huerta-Cepas, M. Simonovic, A. Roth, A. Santos, K.P. Tsafou, M. Kuhn, P. Bork, L.J. Jensen, C. von Mering, STRING v10: protein–protein interaction networks, integrated over the tree of life, Nucleic Acids Res. 43 (2015) D447–D452. doi:10.1093/nar/gku1003.

[49] V. Ettorre, P. De Marco, S. Zara, V. Perrotti, A. Scarano, A. Di Crescenzo, M. Petrini, C. Hadad, D. Bosco, B. Zavan, L. Valbonetti, G. Spoto, G. Iezzi, A. Piattelli, A. Cataldi, A. Fontana, In vitro and in vivo characterization of graphene oxide coated porcine bone granules, Carbon N. Y. 103 (2016) 291–298. doi:10.1016/j.carbon.2016.03.010.

[50] E. Baldi, M. Luconi, L. Bonaccorsi, C. Krausz, G. Forti, Human sperm activation

during capacitation and acrosome reaction: role of calcium, protein phosphorylation and lipid remodelling pathways., Front. Biosci. 1 (1996) d189–205. http://www.ncbi.nlm.nih.gov/pubmed/9159227 (accessed February 28, 2019).

[51] N.M. Chimote, N.N. Chimote, N.M. Nath, B.N. Mehta, Transfer of spontaneously hatching or hatched blastocyst yields better pregnancy rates than expanded blastocyst transfer., J. Hum. Reprod. Sci. 6 (2013) 183–8. doi:10.4103/0974-1208.121420.

[52] Y. Gur, H. Breitbart, Mammalian sperm translate nuclear-encoded proteins by mitochondrial-type ribosomes., Genes Dev. 20 (2006) 411–6. doi:10.1101/gad.367606.

[53] X. Ren, X. Chen, Z. Wang, D. Wang, Is transcription in sperm stationary or dynamic?, J. Reprod. Dev. 63 (2017) 439–443. doi:10.1262/jrd.2016-093.

[54] N. Bernabò, M.R. Sanchez, L. Valbonetti, L. Greco, G. Capacchietti, M. Mattioli, B. Barboni, Membrane Dynamics of Spermatozoa during Capacitation: New Insight in Germ Cells Signalling, in: Germ Cell, InTech, 2018. doi:10.5772/intechopen.69964.

[55] B.M. Gadella, A. Boerke, An update on post-ejaculatory remodeling of the sperm surface before mammalian fertilization, Theriogenology. 85 (2016) 113–124. doi:10.1016/J.THERIOGENOLOGY.2015.07.018.

[56] J. Chen, G. Zhou, L. Chen, Y. Wang, X. Wang, S. Zeng, Interaction of Graphene and its Oxide with Lipid Membrane: A Molecular Dynamics Simulation Study, J. Phys. Chem. C. 120 (2016) 6225–6231. doi:10.1021/acs.jpcc.5b10635.

[57] M. Tang, B.-J. Liu, S.-Q. Wang, Y. Xu, P. Han, P.-C. Li, Z.-J. Wang, N.-H. Song, W. Zhang, C.-J. Yin, The role of mitochondrial aconitate (ACO2) in human sperm motility, Syst. Biol. Reprod. Med. 60 (2014) 251–256. doi:10.3109/19396368.2014.915360.

[58] W. Cao, H.K. Aghajanian, L.A. Haig-Ladewig, G.L. Gerton, Sorbitol can fuel mouse sperm motility and protein tyrosine phosphorylation via sorbitol dehydrogenase., Biol. Reprod. 80 (2009) 124–33. doi:10.1095/biolreprod.108.068882.

[59] T.M.D. Nguyen, Y. Combarnous, C. Praud, A. Duittoz, E. Blesbois, Ca2+/Calmodulin-Dependent Protein Kinase Kinases (CaMKKs) Effects on AMP-Activated Protein Kinase (AMPK) Regulation of Chicken Sperm Functions., PLoS One. 11 (2016) e0147559. doi:10.1371/journal.pone.0147559.

[60] T.M. Lakowski, G.M. Lee, M. Okon, R.E. Reid, L.P. Mcintosh, Calcium-induced folding of a fragment of calmodulin composed of EF-hands 2 and 3, (n.d.). doi:10.1110/ps.072777107.

[61] M. Ikura, Calcium binding and conformational response in EF-hand proteins., Trends Biochem. Sci. 21 (1996) 14–7. http://www.ncbi.nlm.nih.gov/pubmed/8848832 (accessed January 17, 2019).

[62] H. Yuan, J. Qi, C. Xing, H. An, R. Niu, Y. Zhan, Y. Fan, W. Yan, R. Li, B. Wang, S. Wang, Graphene-Oxide-Conjugated Polymer Hybrid Materials for Calmodulin Sensing by Using FRET Strategy, Adv. Funct. Mater. 25 (2015) 4412–4418. doi:10.1002/adfm.201501668.

[63] K. Kenry, K.P. Loh, C.T. Lim, Molecular interactions of graphene oxide with human blood plasma proteins, Nanoscale. 8 (2016) 9425–9441.

doi:10.1039/C6NR01697A.

[64] R.C. Tuckey, Progesterone synthesis by the human placenta, Placenta. 26 (2005) 273–281. doi:10.1016/j.placenta.2004.06.012.

Figure captions

Figure 1. Experimental design. The three main experimental groups and the four control conditions are shown. From left to right: control group (CTRL), spermatozoa unbound (BOEC), spermatozoa released from BOEC by P4 action (BOEC-P4), spermatozoa just treated with P4 without BOEC (P4), spermatozoa released from BOEC by GO action, and just GO-treated spermatozoa without BOEC (GO). All the sperm experimental groups were subjected to BSP, PKA and protein tyrosine phosphorylation analysis by Western Blot, and to lipidomic and proteomic analysis by ICM-MS, while only CTRL, BOEC-P4 and BOEC-GO groups were also used to carry out IVF and blastocyst yield (BY) analysis and FRAP experiments.

Figure 2. Assessment of sperm membrane fluidity by Fluorescence Recovery After Photobleaching (FRAP). Scatter plot shows calculated diffusion coefficient (CDC) of control group, GO-released spermatozoa (BOEC-GO) and P4-released spermatozoa (BOEC-P4). CDC: calculated diffusion coefficient (cm2/sec) x109. Means and percentiles 25 and 75% are represented (n=6 replicates, $p<0.05$).

Figure 3. BSP-1, -3, -5 abundance. Histogram exhibits the comparison of BSP-1,-3 and -5 abundance on spermatozoa control (CTRL), spermatozoa unbound or released after a short period of binding and release, spermatozoa released by P4 (BOEC-P4), just-treated P4 spermatozoa (P4), released by GO (BOEC-GO) and just GO-treated (GO) in terms of mean ± SD (n= 3 replicates).

Figure 4. Phosphorylated Ser/Thr residues by PKA and protein tyrosine phosphorylation. (A) Means ± SEM of PKA activity in spermatozoa unbound or released after a short period of binding and release, spermatozoa released by P4 (BOEC-P4), just-treated P4 spermatozoa (P4), released by GO (BOEC-GO) and just GO-treated

(GO) **(B)** Means ± SEM of protein tyrosine phosphorylation levels in the same groups (n=3 replicates for both histograms, p>0.05).

Figure 5. Distribution of differential lipids and proteins between the experimental groups. Venn diagrams confronting the differential m/z identified by ICM-MS for lipidomic (A,B) and proteomic (C,D) profiles. CTRL: control spermatozoa; BOEC-GO: spermatozoa bound to BOECs and then released by GO; GO: spermatozoa just treated with GO; BOEC-P4: spermatozoa bound to BOECs and then released by P4 action. (http://bioinformatics.psb.ugent.be/webtools/Venn/).

Figure 6. Hierarchical clustering and Principal Component Analysis (PCA) of differential lipids and proteins in spermatozoa. Hierarchical clustering (top) and PCA (bottom) of differentially abundant masses among the three main experimental groups (CTRL, BOEC-GO, GO) for lipidomic (A) and proteomic (B) analyses. CTRL: control spermatozoa; BOEC-GO: spermatozoa bound to BOECs and then released by GO; GO: spermatozoa just treated with GO. On the color bar, red is the high spectral count and green is the low count. Patterns of m/z signals were classified into clusters by hierarchical clustering based on different phenotypes of sperm cells.

Figure 7. Protein-protein interaction network. Network illustrating the associations between the proteins that matched with the peptides identified (https://string-db.org/)

Table captions

Table 1. In vitro fertilization and embryo development outcomes. Means ± SD of cleavage rate at Day 2, blastocyst rates at Days 7 and 8 pi and hatching at Day 8 of bovine in-vitro matured oocytes with control spermatozoa (CTRL), spermatozoa released after P4 (BOEC-P4) and GO (BOEC-GO) action. COCs: total number of

cumulus oocyte complexes (COCs); % cleavage from the total COCs number; % of blastocyts from the cleaved embryos; % hatching/hatched from the number of blastocyst at Day 8. *Significantly different compared to CTRL ($p<0.05$).

Supplementary Data

Supplementary Material 1. Spermatozoa released by heparin, P4 or GO action. Mean ± SD of spermatozoa released by P4 (BOEC-P4) and GO (BOEC-GO), normalized with the number of spermatozoa released by Heparin (BOEC-HEP), considered to release the 100% of sperm cells (n=5 replicates).

Supplementary Material 2. Representative spectra from lipidomic and proteomic analysis by ICM-MS. A) Representative spectra of the CTRL group derived from lipidomic analysis with m/z ranging from 400 to 900; B) Representative spectra of the CTRL group derived from proteomic analysis with m/z ranging from 1,000 to 20,000. Both spectra were obtained after calibration and application of lock mass.

Supplementary Material 3. **List of masses found in lipidomic analysis by ICM-MS**. List of masses obtained by confronting the main experimental groups (CTRL, BOEC-GO, GO and BOEC-P4) in the lipidomic analysis after the spectral processing and analysis performed with ClinProTools v3.0 software. Columns from left to right: mass (m/z); area under the curve (AUC); p value obtained after Kruskal-Wallis analysis (PWKW); average value of the first group (Ave1); average value of the second group (Ave2); fold change of group 1 against group 2 (FC1/2); fold change of group 2 against group 1 (FC2/1); standard deviation of group 1 (StdDev1); standard deviation of group 2 (StdDev2); coefficient of variation group 1 (CV1); coefficient of variation

group 2 (CV2). Color code: red, p value < 0.01; blue, p value < 0.01 and area under the curve (AUC) > 0.8; green, p value < 0.01, AUC > 0.8 and FC > 1.5 or < 0.67.

Supplementary Material 4. List of masses found in proteomic analysis by ICM-MS. List of masses obtained by confronting the main experimental groups (CTRL, BOEC-GO, GO and BOEC-P4) in the proteomic analysis after the spectral processing and analysis performed with ClinProTools v3.0 software. Columns from left to right: mass (m/z); area under the curve (AUC); p value obtained after Kruskal-Wallis analysis (PWKW); average value of the first group (Ave1); average value of the second group (Ave2); fold change of group 1 against group 2 (FC1/2); fold change of group 2 against group 1 (FC2/1); standard deviation of group 1 (StdDev1); standard deviation of group 2 (StdDev2); coefficient of variation group 1 (CV1); coefficient of variation group 2 (CV2). Color code: red, p value < 0.01; blue, p value < 0.01 and area under the curve (AUC) > 0.8; green, p value < 0.01, AUC > 0.8 and FC > 1.5 or < 0.67.

Supplementary Material 5. List of identified lipids among the differential *m/z* detected by ICM-MS. Observed MALDI masses (m/z) ICM-MS, theoretical mass (Da) and % of delta mass are exposed. Fold changes (FC) are ratios of mean normalized intensity values between experimental groups: spermatozoa released from BOEC by GO action (BOEC-GO), treated with GO without BOEC (GO) or just manipulated (CTRL).

Supplementary Material 6. List of identified proteins among the differential *m/z* detected by ICM-MS. Observed MALDI masses (m/z) ICM-MS, theoretical mass (Da) and % of delta mass are exposed. Fold changes (FC) are ratios of mean normalized intensity values between experimental groups: spermatozoa released from BOEC by GO action (BOEC-GO), treated with GO without BOEC (GO) or just manipulated (CTRL).

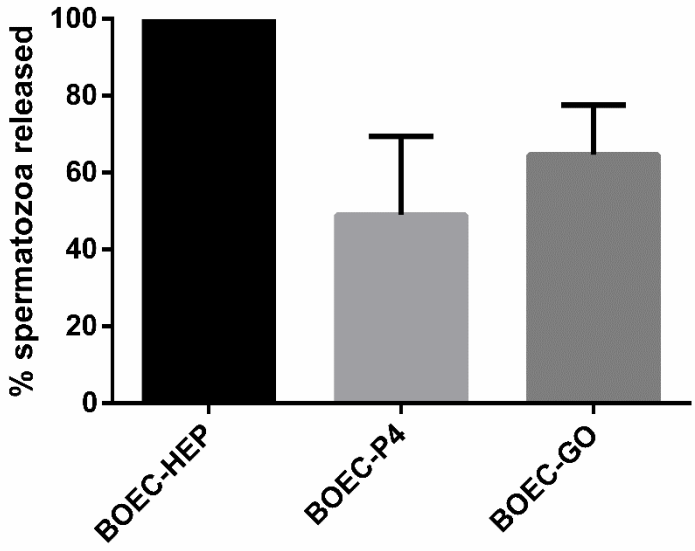

Supplementary Material 1. Spermatozoa released by heparin, P4 or GO action. Mean ± SD of spermatozoa released by P4 (BOEC-P4) and GO (BOEC-GO), normalized with the number of spermatozoa released by Heparin (BOEC-HEP), considered to release the 100% of sperm cells (n=5 replicates).

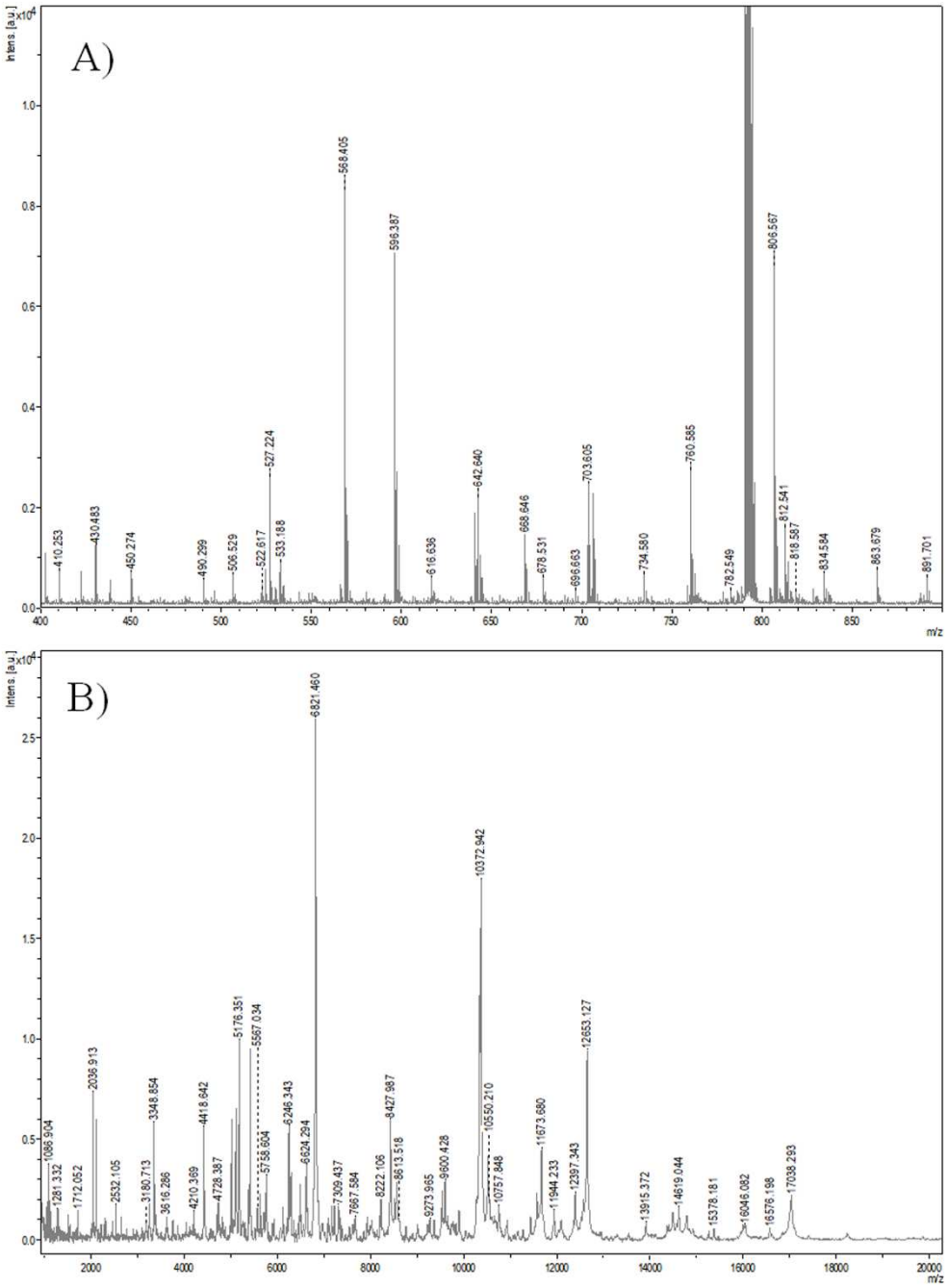

Supplementary Material 2. Representative spectra from lipidomic and proteomic analysis by ICM-MS. A) Representative spectra of the CTRL group derived from lipidomic analysis with m/z ranging from 400 to 900; B) Representative spectra of the CTRL group derived from proteomic analysis with m/z ranging from 1,000 to 20,000. Both spectra were obtained after calibration and application of lock mass.

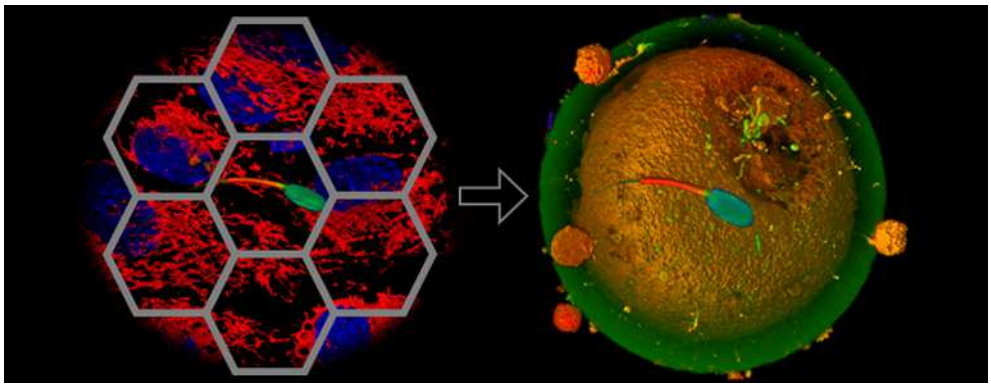

Graphical abstract